

**Palestine Polytechnic University**



**College of Engineering and Technology  
Mechanical Engineering Department  
Mechatronics Engineering**

**Graduation Project**

**Integrated Crane Conveyor System (ICCS)**

**Project Team**

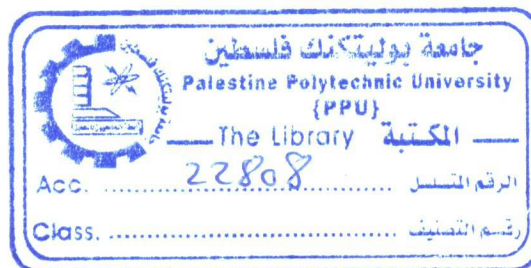
**HAYTHAM ZUGHAIR SAED ABU RAYYAN**

**Project Supervisor**

**Eng. MAJDI ZALLOUM**

**Hebron-Palestine**

**June-2008**



**Palestine Polytechnic University  
(PPU)**

**Hebron-Palestine**

**Integrated Crane Conveyor System (ICCS)**

**Project Team**

**SAED ABU RAYYAN  
HAYTHAM ZUGHAIR**

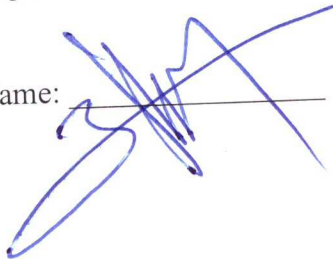
**Project Supervisor**

**Eng. MAJDI ZALLOUM**

According to the project supervisor and according to the agreement of the testing committee members, this project is submitted to the Department of Mechanical Engineering at college of engineering and technology in partial fulfillment of the requirements of the bachelor's degree.

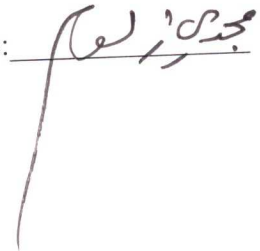
Department Head Signature

Name: \_\_\_\_\_



Supervisor Signature

Name: \_\_\_\_\_



June -2008

**Dedication:**

*A very special dedication To our parents who  
meant the most to us.*

*To all of our friends...*

*To the souls of Martyrs ...*

*To who carry candle of science  
To light his avenue  
Of life ...*

## **Acknowledgment**

We want to thank our university and its teaching staff, for their guidance of us in order to get the wide, and the most important information and knowledge in different fields.

We wish to present special thanks to our supervisor in this project Eng. MAJDI ZALLOUM, who didn't prevent any information and supporting ideas that relate to this project or other fields.

We wish to present special thanks to Eng. KHALED TMIEZI Eng. AHMAD TAHBOUB, Eng. AMEEN AL-JOUBEH and Eng BAHAA' ALWOHOOSH, who didn't prevent any information and supporting ideas that relate to this project or other fields.

## **ABSTRACT**

### **Integrated Crane Conveyor System(ICCS)**

#### **Project Team**

**SAED ABU RAYYAN**

**HAYTHAM ZUGHAIR**

**Palestine Polytechnic University-2008  
(PPU)**

#### **Project Supervisor:**

**Eng. MAJDI ZALLOUM**

In this project synchronization will be achieved between two mechanical systems to produce a mechatronics system. The two systems are a conveyor and a Jib crane , the crane will lift an iron specimen from the conveyor by the magnetic field approach and put it in the desired position, while the Conveyor will bring the next part and so on. Computer will be used to control the operation and suitable sensors will be used to give information about the two systems, also some needed circuit are used to control the system.

This project based on two mechanical systems that have been made in Palestine Polytechnic University by a mechatronics graduated students and we will benefit from their work on this two subjects by studying the mathematical model of both of them and study the text books that have been written in this field.

The most important thing in this work is the final part, in which the implementation of the practical procedure will be started after the theoretical study for this project is finished.

## Table of contents

Subject	Page Number
Project title	i
Evaluation of the project	ii
Dedication	iii
Acknowledgment	iv
Abstract	v
Table of contents	vi
List of figures	ix
List of tables	xi
Appendix A	85
Appendix B	89
Appendix C	91
References	114

Chapter One	Introduction	
1.1	Project Description	1
1.2	Automation Introduction	2
1.3	Aims of project	3
1.4	The smart Conveyor	3
1.5	The assisted Jib crane	5
1.6	Work Principle and Conceptual Design	7
1.7	Mechatronics design approach	9
1.8	Estimated Cost	11
1.9	Project Schedule	12

## **Chapter Two      Mathematical Modeling**

2.1	Introduction	13
2.2	Smart Conveyor	13
2.2.1	Mathematical Model of the Conveyor	13
2.2.2	State Space Model	16
2.2.3	Conveyor Load and Part Specifications	17
2.3	Mathematical Modeling of the Jib crane	20
2.3.1	Derivation of the model	21
2.3.2	State Space Model of the Crane	25
2.3.2.1	Linearization	28
2.3.2.1.1	Linearization around the stationary state	28
2.3.2.1.1	Calculating the operating points of the Jib Crane System	31
2.3.3	Transfer Function of The Jib Crane	34
2.4	Lifting Force	38
2.4.1	Introduction to electromagnet	38
2.4.2	Electromagnets and permanent magnets	38
2.4.3	Magnetic Force Analysis	39
2.5	Statics and mechanical analysis	41

## **Chapter Three      Actuators and Sensors**

3.1	Introduction	42
3.2	Motors Selection	42
3.2.1	Motor of the Conveyor	43
3.2.2	Motor of the rotational motion of the Jib crane	44
3.2.3	Translational Motion Motor of the Jib crane	46

3.2.4	Hoisting Motor	48
3.3	Sensors	48
3.3.1	Part detecting sensor	48
3.3.2	Angle of Rotation Sensing	50
3.3.3	Trolley Radial Distance Sensing	52
3.3.4	Hoisting Distance Sensing	56

#### **Chapter Four                    Interfacing System**

4.1	Introduction	58
4.2	Interfacing	58
4.2.1	Digital Isolation	58
4.2.2	Rotational Motor Interfacing	60
4.2.3	Electrical Switches	61
4.3	Data Acquisition Card	62
4.4	Real Time Windows Target	64

#### **Chapter Five                    Control and Synchronization**

5.1	Introduction	67
5.2	Rotational Motor Control	68
5.2.1	PID Controller Design	68
5.2.2	Mechanical Disturbance Rejection	75
5.3	Conveyor Motor Control	76
5.4	Synchronization	77
5.4.1	Stateflow Method Definition	77
5.4.2	Stateflow Diagram	78



## List of figures

Figure		Page Number
Figure(1.1)	Integrated Crane-Conveyor System	2
Figure(1.2)	Components of belt conveyor	4
Figure(1.3)	Conceptual design at $\theta = 0^\circ$	5
Figure(1.4)	Jib crane Design	6
Figure(1.5)	Block diagram of the system	8
Figure(1.6)	Mechatronics elements	9
Figure(1.7)	Mechatronics design approach	11
Figure(2.1)	Free body diagram for one part	14
Figure(2.2)	The part dimensions(cm)	20
Figure(2.3)	A 3D model of a rotary crane	22
Figure(2.4)	Oscillation angles of the load: $\phi(t)$ and $\theta(t)$	23
Figure(2.5)	Magnetic lifting force	40
Figure(3.1)	Force on the part	43
Figure(3.2)	Load motor connection	45
Figure(3.3)	Motion of the trolley	47
Figure(3.4)	Inductive proximity sensor	49
Figure(3.5)	Sensor mounting	50
Figure(3.6)	Potentiometer	51
Figure(3.7)	Potentiometer as a Voltage Divider	51
Figure(3.8)	Ultrasonic Sensors	54
Figure(3.9)	Sensor mounting and conical beam	55
Figure(3.10)	Detailed sensor mounting	56
Figure(3.11)	Sensor mounting to measure hoisting distance	57
Figure(4.1)	An optocoupler	59
Figure(4.2)	Driving circuit	60

Figure(4.3)	Relay principle	61
Figure(4.4)	Solid state relay	62
Figure(4.5)	PCI-6024E DAQ card	64
Figure(5.1)	PID controller block diagram	68
Figure(5.2)	Closed loop system block diagram	69
Figure(5.3)	Uncompensated system root locus	71
Figure(5.4)	Calculating PD zero location	71
Figure(5.5)	PD compensated system root locus	72
Figure(5.6)	PID compensated system root locus	73
Figure(5.7)	Step response for PID compensated system	73
Figure(5.8)	Desired step response	74
Figure(5.9)	Worm gear	75
Figure(5.10)	On-off control	76
Figure(5.11)	Stateflow block	77
Figure(5.12)	The stateflow diagram	79
Figure(6.1)	The magnet	81
Figure(6.2)	Inductive proximity sensor	82
Figure(A.1)	DC motor schematic	86
Figure(A.2)	A typical equivalent mechanical load	87
Figure(A.3)	Torque-speed curve of a DC Motor	88
Figure(B.1)	Simulink Program	90

## List of Tables

Table		Page Number
Table(1.1)	Estimated cost	11
Table(1.2)	Project plan for the first semester	12
Table(1.3)	Inertias of rotating parts	45
Table(5.1)	Symbolizing stateflow variables	78
Table(A.1)	Experimental results	88

# **Chapter One**

## **Introduction**

### **1.1 Project Description**

Integrated Crane-Conveyor System (ICCS), is a combination of two mechanical systems which are a jib crane and conveyor (figure(1.1)) that performs a specific tasks which are lifting, moving and putting a steel part to a desired position. This operation will be controlled by a computer control system.

This system has a great effect on manufacturing especially, in automated material handling system which is in charge of moving materials in the factory effectively. It plays a big role in saving time, effort and labor.

This system represents a computer manufacturing system (CMS) from the second level which we have two mechanical systems that are connected to the central computer through a data acquisition card (DAC).

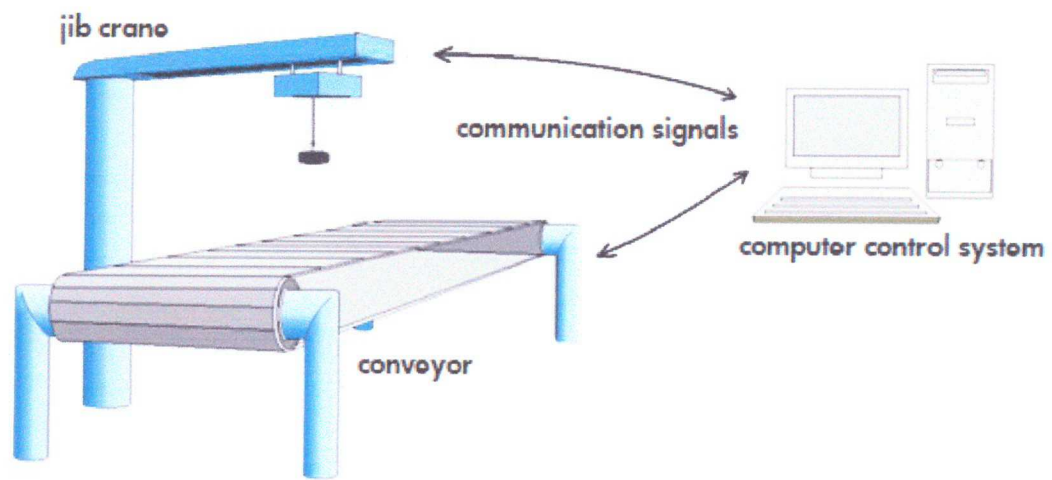


**Figure (1.1):** Integrated Crane-Conveyor System

## 1.2 Automation Introduction

Automation is the technology by which a process or procedure is accomplished without human assistance. It is implemented using a program of instructions combined with a control system that executes the instruction. To automate a process, power is required, both to drive the process itself and to operate the program and control system. Although automation can be applied in a wide variety of areas, it is most closely associated with the manufacturing industries.

An automated system consists of three basic elements: power to accomplish the process and operate the system, a program of instructions to direct the process, and a control system to actuate the instructions. All systems that qualify as being automated include these three basic elements in one form or another. [3]

In our project we will construct an automated system includes two mechanical systems which are a belt conveyor and jib crane, these two systems are previous graduation projects.

### **1.3 Aims of Project**

1. To make synchronization between two mechanical systems to achieve the automation.
2. To achieve a computer manufacturing system from the second level.
3. To make a complete mechatronics system based on four parts: mechanical, electrical, computer science and information technology.
4. To achieve optimization with best design and low cost by using mechatronics design approach.

### **1.4 The Conveyor**

Conveyors are used when material must be moved in relatively large quantities between specific locations over a fixed path. The fixed path is implemented by a track system, which may be in-the-floor, above-the-floor. conveyors divided into two basic categories powered and non-powered. In powered conveyors, the power mechanism is contained in the fixed path, using chains, belt, rotating rolls, or other device to load along the path. Powered conveyors are commonly used in automated material transport systems in manufacturing plants, and distribution center. In non-powered

conveyors, materials are moved either manually by human workers who push the loads along the fixed path or by gravity from one elevation to a lower elevation.

In this project the conveyor which is to be used is belt conveyor figure(1.2), the belt is made of reinforced rubber, so that it possesses high flexibility but low extensibility. At one end of the conveyor is a drive roll that powers the belt. The flexible belt is supported by a frame that has support slider along its forward path. [3]

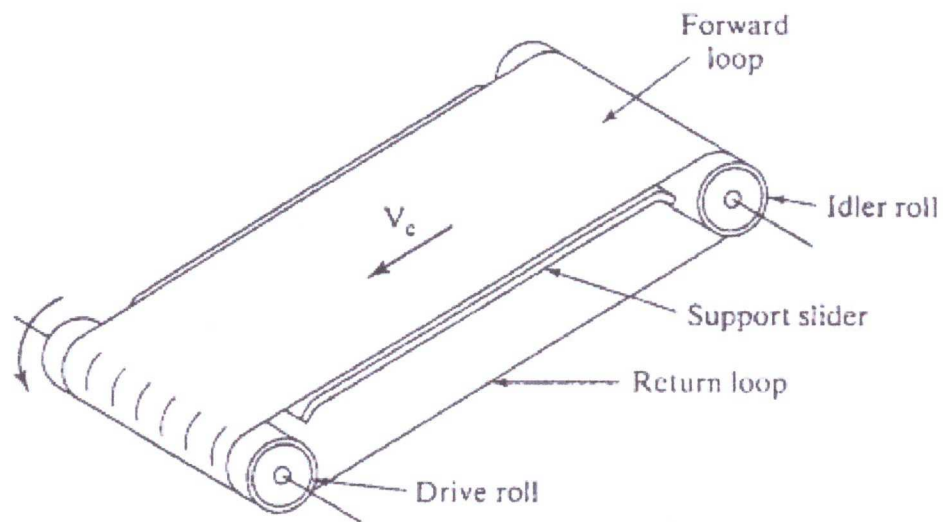


**Figure (1.2):** Components of belt conveyor

A prototype of the conveyor shown in figure (1.3), the conveyor will build of 95cm length, and with controllable variable angles ( $\theta$ ) from 0 to 40°, by this length and the variable angles that will give a variety of moving materials, which means moving material from the ground to the truck, or from the ground to the first, and second floor, and that the market which needs exactly. Also the conveyor will be a belt conveyor type and that because the belt has good coefficient friction which help of no materials slipping also the belt has low cost. Also the conveyor will be a

continuous motion conveyor type and has a constant velocity when traveling materials from one place to another. The conveyor will move vertically using screw mechanism, uses this mechanism because it has low cost compared with hydraulic system. **But in our project we are intended in ( $\theta=0$ ).** [1]

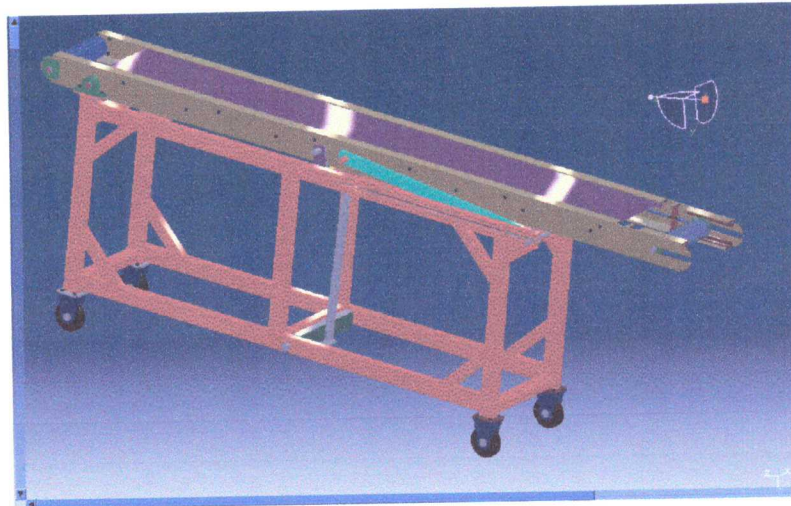


**Figure (1.3):** Conceptual design at  $\theta = 0^\circ$

### 1.5 The Jib Crane

Jib crane can be considered as a kind of Bridge cranes. Jib cranes feature a horizontal bridge girder equipped with a pulley that can move across the length of the bridge. The difference between jib and traditional bridge cranes is the supports. Whereas bridge cranes feature multiple supporting girders, a jib crane only has one as shown in Figure (1.4). That solitary support then pivots allowing the jib crane to service a large, circular area without taking up a lot of space. Because they only have one support, however, they cannot lift as much weight as other overhead cranes.



Jib Crane consists of a horizontal load supporting boom, which is attached to a pivoting vertical column that is either free standing or building mounted. They enable lifting and lowering of a load within a fixed arc of rotation. The jib crane that will be designed in this project will be of the same components as detailed in Figure (1.4). [2]

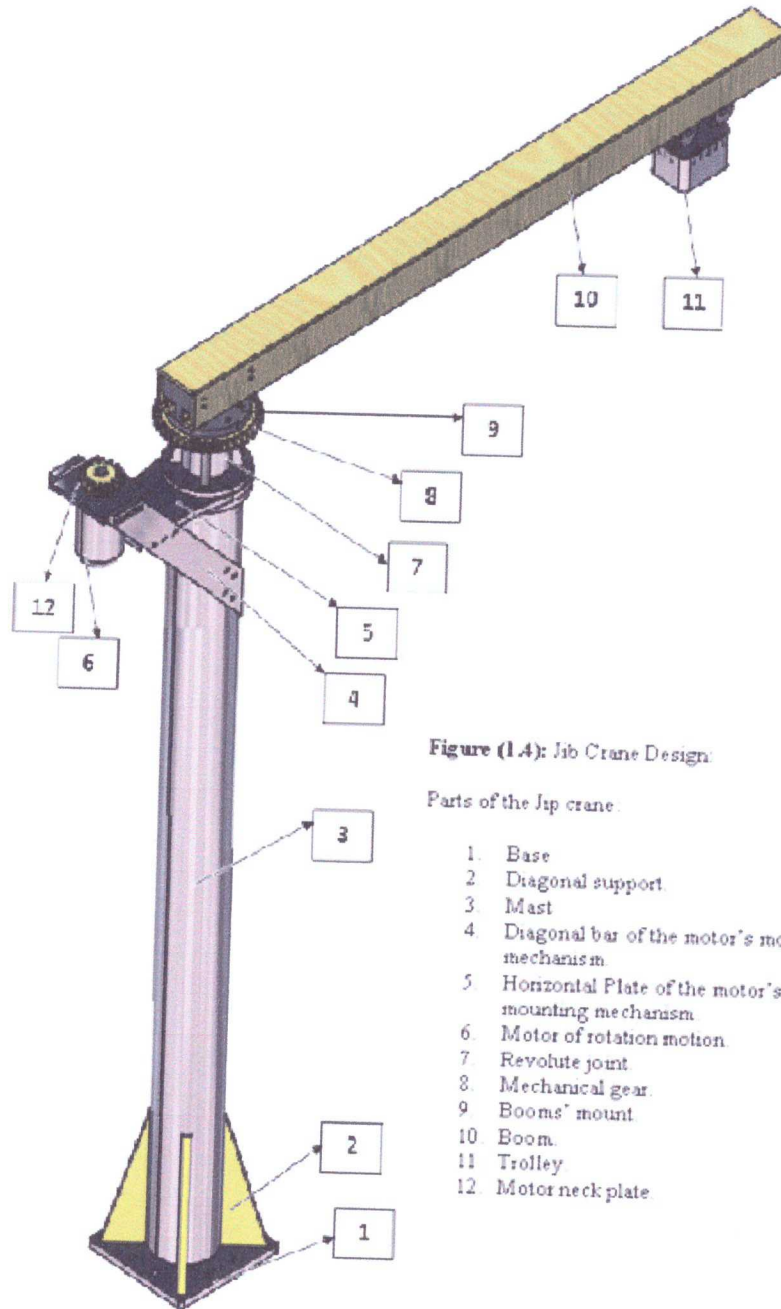


Figure (1.4): Jib Crane Design

Parts of the Jip crane

1. Base
2. Diagonal support
3. Mast
4. Diagonal bar of the motor's mounting mechanism
5. Horizontal Plate of the motor's mounting mechanism
6. Motor of rotation motion
7. Revolute joint
8. Mechanical gear
9. Booms' mount
10. Boom
11. Trolley
12. Motor neck plate

## **1.6 Work Principle and Conceptual Design**

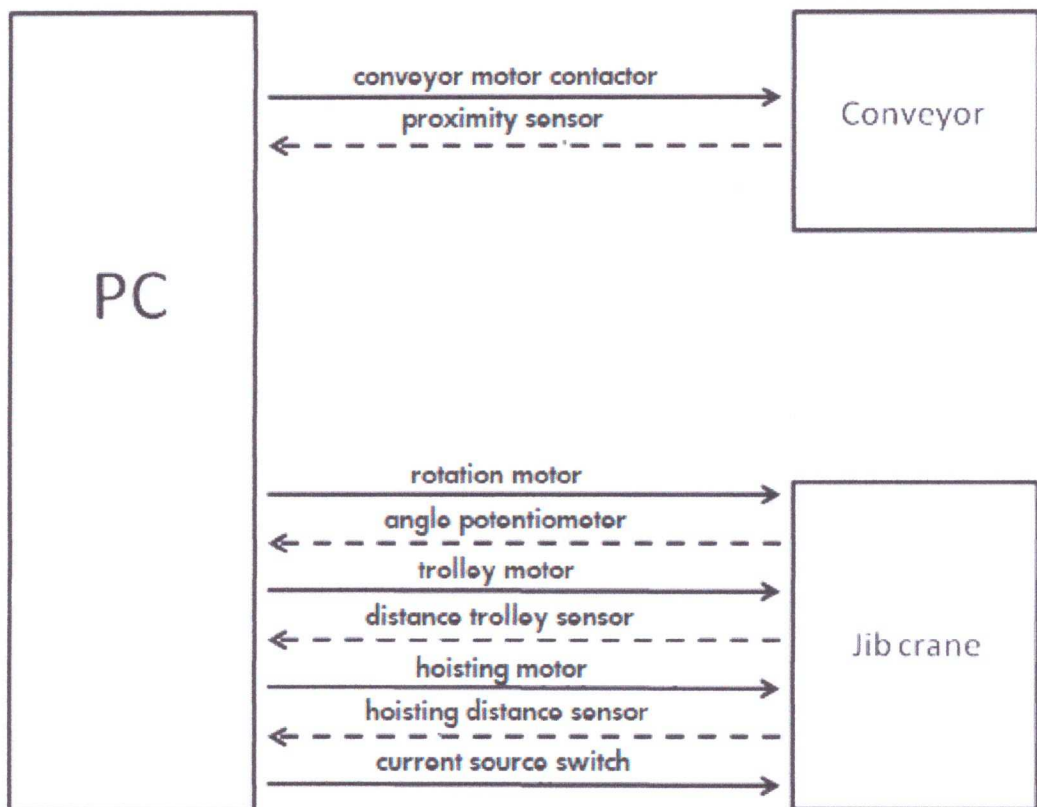
The job of this system is to lift a part from the conveyor and move it to specific position and put it in that position. First the computer will receive a signals from sensors about system status. This information is important to make the system ready to start working by going to the initial position.

When the system starts, the conveyor will start moving the part until it reaches a position from where the crane will lift it. A signal will be sent from a proximity sensor to computer informed that the part has arrived, the computer sends a signal that stops the motor of the conveyor. A weight sensor will check the weight of part whether it matches the standard or not.

The computer gives an order to the jib crane to come to the position on the conveyor from which the part will be lifted. The crane position is determined by three parameters which can be detected by three sensors, those sensors will measure angle of rotation , the trolley position and the hoisting distance. The angel of rotation can be measured with a potentiometer. Trolley's position and hoisting can be measured using a distance sensor (laser, ultrasonic).

When the crane reaches this position the hoist will go downward to the part, after the computer checks the position of the crane determined by three parameters which are mentioned above, if the crane is in the right position the computer sends a signal to switch on the current source to supply the coil with current to generate the sufficient magnetic force needed to lift the part.

To check that the crane lifted the part or not , the part detecting sensor(proximity) will send a signal to the computer informs that is no part at that position. After that the crane will lift the part then it will move the part to the desired position while that the conveyor motor is activated by a signal sent from the computer so the conveyor brings the next part and so on(figure(1.5)).

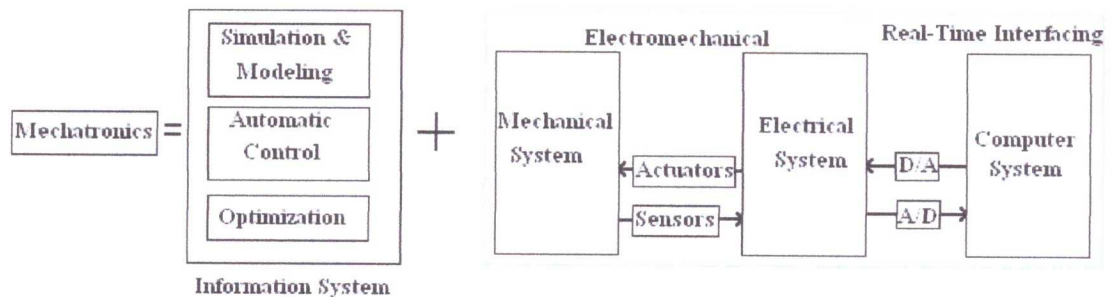


**Figure(1.5):** Block diagram of the system.

## 1.7 Mechatronics Design Approach

Mechatronics is a methodology used for the optimal design of electromechanical products; Mechatronics system is multi-disciplinary embodying four fundamental disciplines: electrical, mechanical, computer science and information technology.

The mechatronics design methodology is based in a concurrent design, instead of traditional or sequential, approach to discipline design, resulting in products with more synergy, this synergy is generated by the right combination of parameters so that this system design offers solutions to all problems in design. A clearer representation (figure 1.6) will show the main parts that a Mechatronics system is composed of. [1]



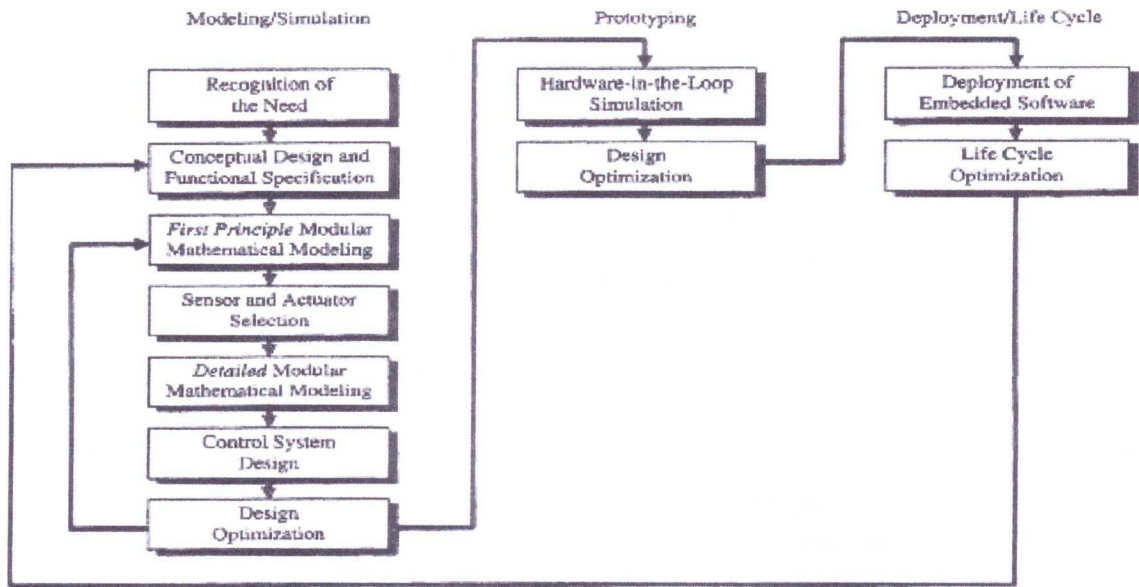
**Figure(1.6):** Mechatronics elements.

To apply the Mechatronics design methodology on our project, we will explain briefly the components of this project to adapt the components of the Mechatronics design methodology.

Any Mechatronics system will contain these components:

1. Mechanical system: that is represented by the smart conveyor and the assisted jib crane.
2. Electrical system: which is represented by the electrical source, actuators, sensors and signal convertors (D/A and A/D) which convert the signals from analog to digital or vice versa. Actuators that are represented with the motors of the two mechanical systems, they convert the electrical energy to the mechanical energy. On the other hand sensors measure important physical states of the system and convert them into electrical signals.
3. Computer system: that is represented by the computer control system(PC) which is connected to the electromechanical system through signal convertors. Data acquisition card (DAC) contains signal convertors and will be in charge of interfacing the electromechanical system to the computer control system.
4. Information system: this part contains three subjects: simulation and modeling, automatic control and optimization. The mathematical modeling of the two systems will be derived in the next chapter, simulation and optimization will be discussed in the forward chapters.

The process of mechatronics design starts with modeling, prototyping and deployment (figure(1.7)).



Figure(1.7): Mechatronics design approach.

### 1.8 Estimated Cost

Table(1.1) shows the estimated cost of the project.

Table(1.1): Estimated cost

Item #	Item	Price (NIS)
1	Data Acquisition Card (DAC)	4000
2	DC Motor	500
3	Magnetic Coil	300
4	3 Sensors	2500
5	Personal computer	1000
6	Other expenses	1000
Grand Total		9300 NIS

## 1.9 Project Schedule

Table (1.2): Project plan for the first semester

Week Activity	1	2	3	4	5	6	7	8	9	10	11	12	13	14	15	16
Choosing Project Title	■	■	■	■	■											
Data Collection						■	■	■								
Smart Conveyor Studying							■	■	■							
Jib Crane Studying										■	■	■				
Coupling & Lifting Mechanism Design							■	■	■	■	■	■	■			
Writing & Printing The Project								■	■	■	■	■	■	■		
Preparing the presentation															■	■

## **Chapter2**

### **Mathematical Model of the Jib crane and the Conveyor**

#### **2.1 Introduction**

In this chapter we will present the mathematical modeling of the two systems, which are previous graduation projects, the first is the smart conveyor and the other one is the Intelligent Power Assisted Jib Crane. Then we will analyze the lifting mechanism, which will be done by generating a magnetic force by passing a current in a coil.

#### **2.2 Smart Conveyor**

##### **2.2.1 Mathematical Modeling of The Conveyor**

Newton's second law will be used to derive the equation of motion of the conveyor, which is,  $\Sigma F = m.a$  , where m: mass of the body, a: acceleration of the body and F: the force acting on the body



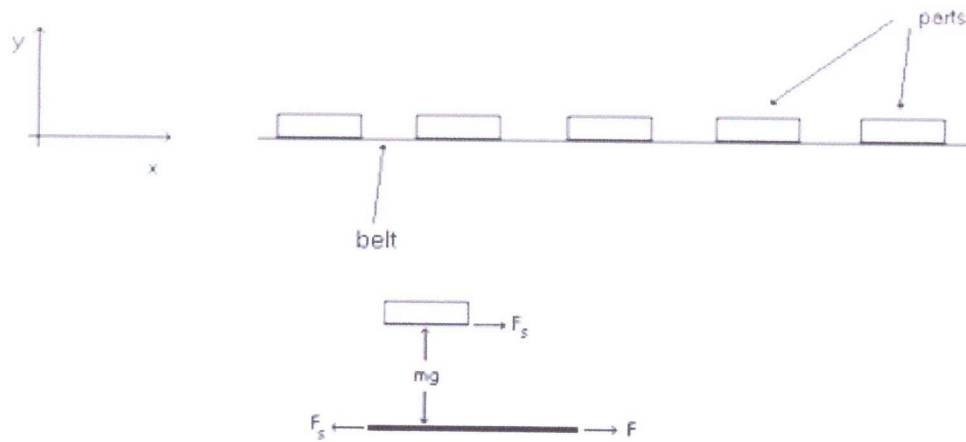


**Figure (2.1):**Free body diagram for one part.

To make the part move on the belt, the friction force must be checked whether or not it can pull the part. If we neglect the friction between the belt and the slider. The friction force between the belt and the part is equal to the normal force multiplied by the static coefficient of friction between the part and the belt, this force must keep the relative velocity between the part and the conveyor zero, so

$$F_f = (m * g)\mu_s > m\ddot{x} \quad (2.1)$$

Where:

$F_s$ : The friction force between the belt and the part

$m$ : The mass of one part

$\mu_s$ : the static coefficient of friction

if divide equation (2.1) by  $m$  we obtain

$$g\mu_s > a \quad (2.2)$$

But  $\mu_s=0.32$  and  $g=9.81\text{m/s}^2$ , so the acceleration must be less than  $3.14\text{ m/s}^2$ . So if the acceleration is less than that value the belt can pull the part and we assume the acceleration to be  $1\text{m/s}^2$ . By applying Newton's second law it can be obtained

$$F = m_{total} * \ddot{x} \quad (2.3)$$

$$m_{Total} = (n \cdot m) + m_{belt} \quad (2.4)$$

Where:

n: the number of parts

m: the part mass

The mass of the belt is small compared to the mass of the part, so it can be neglected, therefore the total mass will be the mass of one part multiplied by the number of parts.

### 2.2.2 State space model

From equation (2.3) we will derive the state space model of the conveyor, let that

$$x_1 = x \quad (a)$$

$$x_2 = \dot{x} \quad (b)$$

From this above equations we conclude that

$$\dot{x}_1 = x_2 \quad (2.5)$$

$$\text{and } \dot{x}_2 = \ddot{x}$$

and substituting in equation (2.1d) we obtain:

$$\dot{x}_2 = \frac{F}{n.m} \quad (2.6)$$

So the state space model is :

$$\dot{x} = \begin{bmatrix} 0 & 1 \\ 0 & 0 \end{bmatrix} \begin{bmatrix} x_1 \\ x_2 \end{bmatrix} + \begin{bmatrix} 0 \\ \frac{1}{n.m} \end{bmatrix} F \quad (2.7)$$

$$y = [1 \quad 0] \begin{bmatrix} x_1 \\ x_2 \end{bmatrix} \quad (2.8)$$

This state space model represents an unstable system since the poles of the system are on origin.

### 2.2.3 Conveyor load and part specifications

The load on the conveyor is modeled by a distributed load equals the number of parts on it multiplied by the mass of each one and divided by the length of the conveyor assuming that the part have the same weight and geometry.

$$p = \frac{n*m*g}{l} \quad (2.9)$$

Where

$p$  : the load per unit length

$g$ : gravity acceleration(9.8m/s<sup>2</sup>)

length of the conveyor and the distance between each part and another, also in the y-direction which is the width of the part we are limited with the width of the conveyor that equals to 12cm , so in this case we are free with the height of the part under the constrain of overturning.

The conveyor is(95cm between the drums' centers), we assume that the distance between each part and the second one is (9cm), so the empty space between the parts is equal to

$$L_{empty\ space} = 6_{number\ of\ empty\ spaces} * 9_{the\ distance\ between\ the\ parts} \quad (2.12)$$

$$L_{empty\ space} = 6 * 9 = 54cm$$

So the total length of the parts is

$$L_{total\ length} = L_{length\ of\ the\ conveyor} - L_{empty\ space} \quad (2.13)$$

$$L_{total\ length} = 95 - 54 = 41cm$$

We assume that the total length is 40cm, So the length of the part if we assumed that we will load 5 parts on the conveyor

$$L_{length\ o\ the\ part} = \frac{L_{total\ length}}{N_{number\ of\ parts}} = \frac{40}{5} = 8\ cm \quad (2.14)$$

To Calculate the width of the part we should consider the width of the conveyor, the width have been measured to be 12cm, we should move away from both sides of the conveyor to give the part a domain to set on the belt of the conveyor without any deviation of its track. so we suppose that we will take from each side 3.25cm as we have suggested, after that we can calculate the width of the part as the following equation:

$$W_{width\ of\ the\ part} = W_{total\ width} - (L_{length\ from\ each\ side} * 2) \quad (2.15)$$

$$W_{\text{width of the part}} = 12 - (3.25 * 2) = 5.5 \text{ cm}$$

So the width of the part is equal to 5.5cm.

After calculating both the length and the of the part, we should evaluate the height of our part to meet our specification, the weight of the part is 1kg as we mentioned before so by using equation (2.10) the volume of the part is:

$$V = \frac{1000g}{7.6g/cm^3} = 131.57 \text{ cm}^3 \quad (2.10.b)$$

By using equation (2.11), the height of the part in the z-direction is:

$$z = \frac{V}{x.y} = \frac{131.57}{8*5.5} = 3 \text{ cm} \quad (2.11.b)$$

so the length of the part is  $41/5 \approx 8$  cm, setting the width 5.5 cm the height will be 3cm ,so the part is  $8 \times 5.5 \times 3$  cm as shown in figure(2.2).

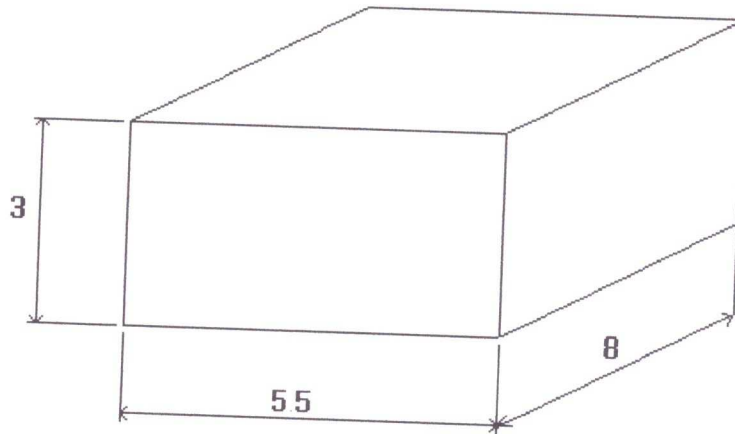


**Figure (2.2):** The part dimensions(cm).

Finally, the part must be checked if it stable on the belt or not, that means will the part overturn or not, so:  $mg(4) > ma(1.5) \rightarrow a < (4/1.5)g \rightarrow a < 26.1867 \text{ m/s}^2$  which is larger than the assumed acceleration( $1 \text{ m/s}^2$ ).

### **2.3 Mathematical modeling of the jib crane[2]**

In this section we will browse the mathematical model of the jib crane, this was made by the pervious students who worked on this project, they used the Lagrange approach. The model of the system is nonlinear so linearization is needed, this was done using Taylor series method using the same operating points calculated by the previous students.

The state space model also will be represented in section, then the transfer functions of the system will be found from the state space model (after linearization), which relate the outputs and the inputs.

#### **2.3.1 Derivation of the model**

Lagrange approach will be used to derive the equation of motion of the jib crane. This approach depends on the conservation of energy principle. The Lagrange's Equation is given in two forms (a) and (b), as shown in Equation (2.16):

$$\frac{d}{dt} \left( \frac{\partial T}{\partial \dot{q}_i} \right) - \frac{\partial T}{\partial q_i} + \frac{\partial V}{\partial q_i} = F_i \dots\dots\dots(a)$$

$$\frac{d}{dt} \left( \frac{\partial \ell}{\partial \dot{q}_i} \right) - \frac{\partial \ell}{\partial q_i} = F_i \dots\dots\dots(b) \tag{2.16}$$

$$\ell = T - V \dots\dots\dots(c) \quad , \quad i = 1, 2, 3, \dots, n$$

Where:

T: Kinetic energy of the system

V: Potential energy of the system

$F_i$  : Non-conservative generalized forces (external applied forces in the direction of generalized coordinates  $q_i$ ).

$q_i$  : Generalized coordinates, or the linear and angular displacements that are used to specify the location of the masses and inertias.

From (b) of the Lagrange Equation can be derived from form (a), by the partial derivation of Equation (2.16.c), then substitution in Equation (2.16.a).

The terms of Equation (2.16.b) can be expressed as:

$\frac{d}{dt} \left( \frac{\partial \ell}{\partial \dot{q}} \right)$  : represents the acceleration term.

$\frac{\partial \ell}{\partial q}$  : represents the gravity term

As shown in Figure (2.3), the crane can be modeled as a vertical cylinder, horizontal boom, and the trolley, this model provides a clear view which helps in developing the equation of motion.

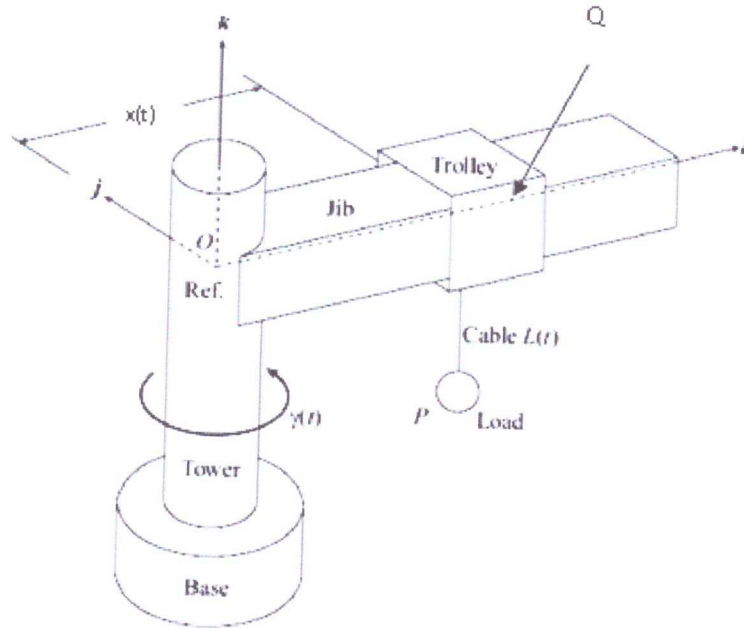


Figure (2.3): A 3D model of a rotary crane.

Now the position vectors of the load and the trolley will be derived, assuming that the trolley is positioned at point Q, which is located at displacement  $x(t)$  from the tower center as in Figure (2.3). The coordinate system that is considered to develop the position vectors is shown in Figure (2.3), so these vectors can be written, as:

$$\begin{aligned} \vec{r}_L &= \{ [x - L \cos(\theta) \sin(\phi)]i + [L \sin(\theta)]j - [L \cos(\theta) \cos(\phi)]k \} \\ \vec{r}_T &= x_i \end{aligned} \tag{2.17}$$



Where  $\vec{r}_L$  is the position vector for the load represented in the three coordinates  $i, j, k$ ,  $\vec{r}_T$  is the position vector of the trolley, and it is represented in the  $i$  coordinate,  $\theta(t)$  is the out-of-plane oscillation angle,  $\phi(t)$  is the in-of-plane oscillation angle, and  $L(t)$  is load line length.

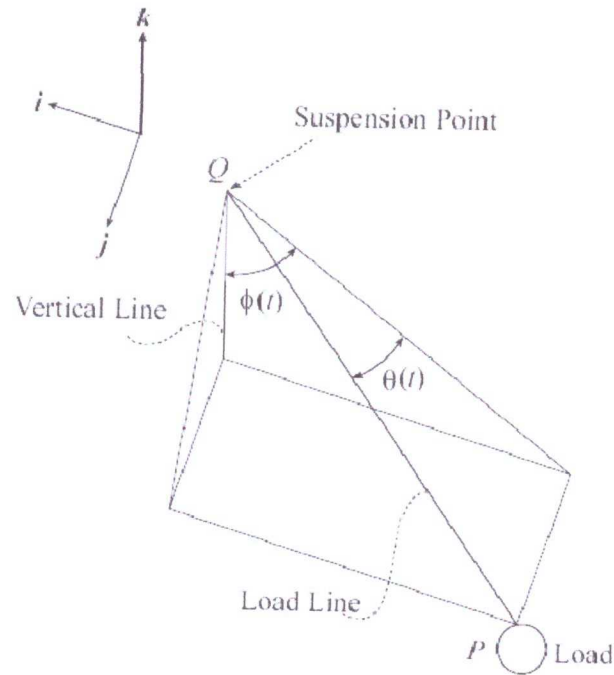


**Figure (2.4):** Oscillation angles of the load:  $\phi(t)$  and  $\theta(t)$ .

The terms in Equation (2.17) are the position components in x, y, and z coordinates, where the load line is projected on the three coordinates.

Considering a constant cable length, such that  $\frac{dL}{dt} = 0$ , the following equations of motion for the system according to the generalized coordinates and generalized forces and moments, can be obtained:

$$\begin{aligned}
& \ddot{\theta} + (x/L \cos(\theta) - \cos(\theta)^2 \sin(\theta) - \sin(\theta)^2 \sin(\phi)) \ddot{\gamma} + (\sin(\theta) \sin(\phi)) \ddot{x}/L \\
& + (\dot{x} \dot{\gamma}/L) \cos(\theta) + (x (\dot{\gamma})^2/L) \cos(2\theta) - (1/4) (\dot{\gamma})^2 L^2 \sin(4\theta) - (1/2) (\dot{\gamma})^2 \sin(2\theta) \\
& - \dot{\gamma} \dot{\phi} \cos(\theta)^2 \cos(\phi) + (1/2) (\dot{\phi})^2 \sin(2\theta) + (g/L) \sin(\theta) \cos(\phi) = 0
\end{aligned} \tag{2.18.a}$$

$$\begin{aligned}
& L \ddot{\phi} \cos(\theta)^2 - (\cos(\theta) \cos(\phi)) \ddot{x} + ((1/2)L \sin(2\theta) \cos(\phi)) \ddot{\gamma} \\
& + L \dot{\gamma} \dot{\theta} (\cos(\phi) \cos(\theta)^2) - L \dot{\phi} \dot{\theta} \sin(2\theta) + L (\dot{\phi})^2 \cos(\phi) \sin(\theta) \\
& + g \cos(\theta) \sin(\phi) = 0
\end{aligned} \tag{2.19.a}$$

$$\begin{aligned}
& (m + M) \ddot{x} - mL \sin(\theta) \ddot{\gamma} + (mL \sin(\theta) \sin(\phi)) \ddot{\theta} - (mL \cos(\theta) \cos(\phi)) \ddot{\phi} \\
& - (M + m)x (\dot{\gamma})^2 - m (\dot{\gamma})^2 L \dot{\theta} \cos(\theta) - 2m \dot{\gamma} \dot{\theta} L \cos(\theta) + 2m \dot{\theta} \dot{\phi} L \sin(\theta) \cos(\phi) \\
& + m (\dot{\theta})^2 L \cos(\theta) \sin(\phi) + mL (\dot{\phi})^2 \cos(\theta) \sin(\phi) = F_x
\end{aligned} \tag{2.20.a}$$

$$\begin{aligned}
& ((m + M)(\dot{x})^2 + J_0 + mL^2 \sin(\theta)^2 - 2mxL \cos(\theta) \sin(\theta) + mL^2 \cos(\theta)^2 \sin(\theta)^2) \ddot{\gamma} \\
& - mL \sin(\theta) \ddot{x} + (mL^2 \sin(\theta)^2 \sin(\phi) - mL^2 \cos(\theta)^2 \sin(\theta) + x mL \cos(\theta)) \ddot{\theta} \\
& + (1/2)mL^2 \sin(2\theta) \cos(\phi) \ddot{\phi} + 2mL^2 (\dot{\theta})^2 \cos(\theta) \sin(2\theta) - mLx (\dot{\theta})^2 \sin(\theta) \\
& - mL^2 (\dot{\theta})^2 \sin(2\theta) \sin(\phi) - 2mLx \dot{\gamma} \dot{\theta} \sin(2\theta) + (1/2)m \dot{\gamma} L^2 \dot{\theta} \sin(4\theta) \\
& + mL^2 \dot{\gamma} \dot{\theta} \sin(2\theta) - 2mL^2 \dot{\theta} \dot{\phi} \sin(\theta)^2 \cos(\phi) + mL^2 \dot{\phi} \dot{\theta} \cos(\theta)^2 \cos(\phi) \\
& - (1/2)mL^2 (\dot{\phi})^2 \sin(2\theta) \sin(\phi) + 2(M + m)x \dot{x} \dot{\gamma} - m \dot{x} \dot{\gamma} L \cos(\theta) \sin(\theta) = T_y,
\end{aligned} \tag{2.21.a}$$

If these equations are considered deeply, we can see that for Equations (2.18.a), (2.19.a) where the generalized coordinates are  $\theta(t)$  and  $\phi(t)$  respectively; are affected by the position, speed and acceleration of the trolley which is represented by  $x(t)$ , and its derivatives, and also by the angular velocity and angular acceleration which is represented by the derivatives of  $\gamma(t)$  supported from the motor of the rotational motion.

Other thing must be mentioned, which is the Coriolis acceleration terms, which produced from the multiplying of two velocities in two different axes, this term is presented in all equations, which means that there is a relative motions with respect to other, that is during the motion of the load on the trolley in one axis, it also that there is motion of the load, or trolley in the other axis.

### 2.3.2 State-Space Model of the Crane

In order to obtain the transfer functions of the linear model of the system, so the system will be presented in the state space model. Since the states are usually selected according to be equal to the number of degrees of freedom or number to the energy-storage elements in the system, the states in the dynamic mechanical systems

are selected to be the displacements and their derivatives, and because each of the four equations is of second order, so the states will be eight, which are:

$$\left. \begin{array}{l} x_1 = \theta(t) \\ x_2 = \phi(t) \\ x_3 = x(t) \\ x_4 = \gamma(t) \\ x_5 = \dot{\theta}(t) \\ x_6 = \dot{\phi}(t) \\ x_7 = \dot{x}(t) \\ x_8 = \dot{\gamma}(t) \end{array} \right\} \quad (2.22)$$

According to these states, their derivatives will be as shown in Equation (2.23):

$$\left. \begin{array}{l} \dot{x}_1 = x_5 \\ \dot{x}_2 = x_6 \\ \dot{x}_3 = x_7 \\ \dot{x}_4 = x_8 \\ \dot{x}_5 = \ddot{\theta}(t) \\ \dot{x}_6 = \ddot{\phi}(t) \\ \dot{x}_7 = \ddot{x}(t) \\ \dot{x}_8 = \ddot{\gamma}(t) \end{array} \right\} \quad (2.23)$$

Substituting these states into Equations (2.18.a), (2.19.a), (2.20.a), (2.21.a), so they will become as follows:

$$\begin{aligned}
& \dot{x}_5 + ((x_3/L) \cos(x_1) - \cos(x_1)^2 \sin(x_1) - \sin(x_1)^2 \sin(x_2)) \dot{x}_8 \\
& + 1/L (\sin(x_1) \sin(x_2)) \dot{x}_7 + x_7 x_8 L \cos(x_1) + x_3 (x_8)^2 L \cos(2x_1) \\
& - (1/4) (x_8)^2 L^2 \sin(4x_1) - (1/2) L^2 (x_8)^2 \sin(2x_1) - x_8 x_6 \cos(x_1)^2 \cos(x_2) \\
& + (1/2) (x_2)^2 \sin(2x_1) + (g/L) \sin(x_1) \cos(x_2) = 0
\end{aligned} \tag{2.18.b}$$

$$\begin{aligned}
& L \dot{x}_6 \cos(x_1)^2 - (\cos(x_1) \cos(x_2)) \dot{x}_7 + ((1/2) L \sin(2x_1) \cos(x_2)) \dot{x}_8 \\
& + L x_8 x_5 (\cos(x_2) \cos(x_1)^2) - L x_6 x_5 \sin(2x_1) + L (x_6)^2 \cos(x_2) \sin x_1 \\
& + g \cos(x_1) \sin(x_2) = 0
\end{aligned} \tag{2.19.b}$$

$$\begin{aligned}
& (m + M) \dot{x}_7 - (mL \sin(x_1)) \dot{x}_8 + (mL \sin(x_1) \sin(x_2)) \dot{x}_5 \\
& - (mL \cos(x_1) \cos(x_2)) \dot{x}_6 - m (x_8)^2 L x_5 \cos(x_1) \\
& (M + m) x_3 (x_8)^2 - 2m x_8 x_5 L \cos(x_1) + 2m x_5 x_6 L \sin(x_1) \cos(x_2) \\
& + m (x_5)^2 L \cos(x_1) \sin(x_2) + mL (x_6)^2 \cos(x_1) \cos(x_2) = F_x
\end{aligned} \tag{2.20.b}$$

$$\begin{aligned}
& ((m + M) (x_3)^2 + J_0 + mL^2 \sin(x_1)^2 - 2m x_3 L \cos(x_1) \sin(x_1)) \\
& + mL^2 \cos(x_1)^2 \sin(x_1)^2 \dot{x}_8 - mL \sin(x_1) \dot{x}_7 + (-mL^2 \sin(x_1)^2 \sin(x_2) \\
& - mL^2 \cos(x_1)^2 \sin(x_1) + mL \cos(x_1) x_3) \dot{x}_5 + ((1/2) mL^2 \sin(2x_1) \cos(x_2)) \dot{x}_6 \\
& + 2mL^2 (x_5)^2 \cos(x_1) \sin(2x_1) - mL x_3 (x_5)^2 \sin(x_1) - mL^2 (x_5)^2 \sin(2x_1) \sin(x_2) \\
& - 2mL x_3 x_8 x_5 \sin(2x_1) + (1/2) mL^2 x_8 x_5 \sin(4x_1) - mL^2 x_8 x_5 \sin(2x_1) \\
& - 2mL^2 x_5 x_6 \sin(x_1)^2 \cos(x_2) + mL^2 x_6 x_5 \cos(x_1)^2 \cos(x_2) \\
& - (1/2) mL^2 (x_6)^2 \sin(2x_1) \sin(x_2) + 2(M + m) x_3 x_7 x_8 - mL x_7 x_8 \cos(x_1) \sin(x_1) = T_y
\end{aligned} \tag{2.21.b}$$

From these equations the following states-derivatives:  $\dot{x}_5, \dot{x}_6, \dot{x}_7, \dot{x}_8$ , can be obtained, since they are of long and non-linear terms the state space representation will be shown after the linearization.

### 2.3.2.1 Linearization

In order to use the equations of motion to obtain the transfer functions, and designing the controller which will control the crane motions, they must be linearized. The method that is used to linearize these Equations is the Taylor series method. However, before showing the linear state space model of the system, this principle will be expressed.

#### 2.3.2.1.1 Linearization Around the Stationary State

If it is assumed that  $x(t)$  changes only in the neighborhood of the stationary state by  $\Delta x$ , the Taylor series expansion is used to calculate  $\Delta \dot{x} = f(\Delta x, \Delta u)$ , so the Taylor series can be expressed as:

$$f(\Delta x, \Delta u) = f(\Delta \bar{x}, \Delta \bar{u}) + \left. \frac{\partial f}{\partial x} \right|_{x=\bar{x}, u=\bar{u}} \Delta x + \left. \frac{\partial f}{\partial u} \right|_{x=\bar{x}, u=\bar{u}} \Delta u + \dots,$$

$$\Delta \dot{x}_i = \sum_{k=1}^n \left( \left. \frac{\partial f_i}{\partial x_k} \right|_{x=\bar{x}, u=\bar{u}} \right) \Delta x_k + \sum_{j=1}^m \left( \left. \frac{\partial f_i}{\partial u_j} \right|_{x=\bar{x}, u=\bar{u}} \right) \Delta u_j \quad (2.24)$$

$$\Delta \dot{x} = A \Delta x + B \Delta u.$$

Where A is System matrix, and B is the Input matrix, and they are given as:

$$A = \sum_{k=1}^n \left( \frac{\partial f_i}{\partial x_k} \right) \Big|_{x=\bar{x}, u=\bar{u}} = \begin{bmatrix} \frac{\partial f_1}{\partial x_1} & \frac{\partial f_1}{\partial x_2} & \dots & \frac{\partial f_1}{\partial x_n} \\ \frac{\partial f_2}{\partial x_1} & \frac{\partial f_2}{\partial x_2} & \dots & \frac{\partial f_2}{\partial x_n} \\ \vdots & \vdots & \dots & \vdots \\ \frac{\partial f_m}{\partial x_1} & \frac{\partial f_m}{\partial x_2} & \dots & \frac{\partial f_m}{\partial x_n} \end{bmatrix}_{x_0, u_0} \quad (2.25)$$

$$B = \sum_{j=1}^m \left( \frac{\partial f_i}{\partial u_j} \right) \Big|_{x=\bar{x}, u=\bar{u}} = \begin{bmatrix} \frac{\partial f_1}{\partial u_1} & \frac{\partial f_1}{\partial u_2} & \dots & \frac{\partial f_1}{\partial u_n} \\ \frac{\partial f_2}{\partial u_1} & \frac{\partial f_2}{\partial u_2} & \dots & \frac{\partial f_2}{\partial u_n} \\ \vdots & \vdots & \dots & \vdots \\ \frac{\partial f_m}{\partial u_1} & \frac{\partial f_m}{\partial u_2} & \dots & \frac{\partial f_m}{\partial u_n} \end{bmatrix}_{x_0, u_0} \quad (2.26)$$

Where the system matrix is called Jacobean, and it is equal to Equation (2.25).

Also the matrices of the output equation which are C and D matrices can be given as:

$$C = \sum_{k=1}^n \left( \frac{\partial y_i}{\partial x_k} \right) \Big|_{x=\bar{x}, u=\bar{u}} = \begin{bmatrix} \frac{\partial y_1}{\partial x_1} & \frac{\partial y_1}{\partial x_2} & \dots & \frac{\partial y_1}{\partial x_n} \\ \frac{\partial y_2}{\partial x_1} & \frac{\partial y_2}{\partial x_2} & \dots & \frac{\partial y_2}{\partial x_n} \\ \vdots & \vdots & \dots & \vdots \\ \frac{\partial y_m}{\partial x_1} & \frac{\partial y_m}{\partial x_2} & \dots & \frac{\partial y_m}{\partial x_n} \end{bmatrix}_{x_0, u_0} \quad (2.27)$$

$$D = \sum_{j=1}^m \left( \frac{\partial y_i}{\partial u_j} \right) \Big|_{x=\bar{x}, u=\bar{u}} = \begin{bmatrix} \frac{\partial y_1}{\partial u_1} & \frac{\partial y_1}{\partial u_2} & \dots & \frac{\partial y_1}{\partial u_n} \\ \frac{\partial y_2}{\partial u_1} & \frac{\partial y_2}{\partial u_2} & \dots & \frac{\partial y_2}{\partial u_n} \\ \vdots & \vdots & \dots & \vdots \\ \frac{\partial y_m}{\partial u_1} & \frac{\partial y_m}{\partial u_2} & \dots & \frac{\partial y_m}{\partial u_n} \end{bmatrix}_{x_0, u_0} \quad (2.28)$$

Where  $\bar{x} = x_0, \bar{u} = u_0$  are the operating points of the physical system. So these points must be determined. There is a definition must be known, that is a point,  $x_0 = \bar{x}$  is an *equilibrium point* of:

$$\square \quad \dot{x} = f(x, u)$$

If  $f(x_0, u_0) = 0$

Where the zero on the right hand side of the equation is a vector of zeros, that is the same dimension as  $x$  and  $f(x, u)$ .

The Equation  $\square \quad \dot{x} = f(x, u)$  can be written in vector form as:

$$\begin{bmatrix} \square \\ x_1 \\ \square \\ x_2 \\ \vdots \\ \square \\ x_n \end{bmatrix} = \begin{bmatrix} f_1(x_1, x_2, \dots, x_n, u_1, u_2, \dots, u_n) \\ f_2(x_1, x_2, \dots, x_n, u_1, u_2, \dots, u_n) \\ \vdots \\ \vdots \\ \vdots \\ f_m(x_1, x_2, \dots, x_n, u_1, u_2, \dots, u_n) \end{bmatrix} \quad (2.29)$$



So in order to solve for the operating or equilibrium points; Equation (2.29) must be equated with zero.

#### 2.3.2.1.2 Calculating the operating points of the jib crane system

As previously mentioned, that the Jacobean matrix represents the system matrix. This matrix and the input matrix are evaluated at the operating or equilibrium points for both; the states, and the interested inputs. These points are evaluated as expressed in section 2.3.2.1.1.

The Equation  $f(x_0, u_0) = 0$  is a non-linear algebraic equation, so in order to solve it, the *Newton-Raphson* and *Levenberg-Marquardt* methods must be used to solve for its roots, which are the operating points  $(x_0, u_0)$ . These methods are numerical methods where they need numerical iteration, so this method needs a computer to do these numerical iterations with supporting software. MATLAB software has a toolbox for optimization, which is a process depends on the numerical iteration in order to get the most optimal and perfect values of the operating points at which the system will be linearized. The optimization term can be defined as

“In mathematics, the term **optimization**, or **mathematical programming**, refers to the study of problems in which one seeks to minimize or maximize a real function by systematically choosing the values of real or integer variables from within an allowed set” .

In our problem we are seeking for minimizing the effect of the states that represent the in-of-plane and out-of-plane angles and their derivatives.

Commonly, the Newton-Raphson method is used to solve for the roots of complicated functions, and it uses the numerical iteration method. This iterative process follows a set of guidelines to approximate one root, considering the function, its derivative, and an initial x-value. The Newton-Raphson method uses an iterative process to approach one root of a function. The specific root that the process locates depends on the initial, arbitrarily chosen x-value. The following equation is used in the iteration process:

$$x_{n+1} = x_n - \frac{f(x_n)}{f'(x_n)} \quad (2.30)$$

Here,  $x_n$  is the current known x-value,  $f(x_n)$  represents the value of the function at  $x_n$ , and  $f'(x_n)$  is the derivative (slope) at  $x_n$ .  $x_{n+1}$  represents the next x-value that must be found. Essentially,  $f'(x)$ ; the derivative represents  $f(x)/dx$ , ( $dx = \Delta x$ ). Therefore, the term  $f(x)/f'(x)$  represents a value of dx. So:

$$\frac{f(x)}{f'(x)} = \frac{f(x)}{f(x)/\Delta x} = \Delta x \quad (2.31)$$

As more iteration is done, dx will be closer to zero.

The operating points in Jib crane problem are determined for all states and for the two inputs, which represents the input torque  $T_\gamma$  from the motor that provides the rotational motion, and the input force from the translational motion. Since x is variable according to the desired position, the matrices A, B, C, and D are determined at the critical point, which is the maximum distance from the center of rotation, and it is assumed to be equal 1m.

The orders that are used to solve for the operating points using the optimal-toolbox under MATLAB, are:

- *fsolve*: this order is used to solve for the roots of nonlinear equations.
- *fminsearch*: finds the minimum of a scalar function of several variables, starting at an initial estimate. This is generally referred to as unconstrained nonlinear optimization.

This operation (numerical iteration) needs starting values for the operating points. These points are selected arbitrarily with considering the physical nature of the system or throughout an information from the system. According to these starting values, the operating points can be convergent or divergent.

In the Jib crane system, as mentioned previously, it is assumed that the linearization will be at the critical point which is at  $x = 1\text{m}$ , and the in-of-plane and out-of-plane angles are needed to be minimized. Other point must be mentioned that is the angular displacement  $\gamma(t)$ , which is represented by  $x_4$  state, doesn't resulted in the equations which are Equations (2.18),(2.19),(2.20),(2.21), so any starting point of this state will be the same value of the operating point for this state, so it is assumed to be equal 1. From this information the starting values are assumed to be:

$$\left\{ \begin{array}{ll} x_1 = 0 & x_5 = 0 \\ x_2 = 0 & x_6 = 0 \\ x_3 = 0.98 & x_7 = 0 \\ x_4 = 0.1 & x_8 = 0 \end{array} \right\} \text{ and } \left\{ \begin{array}{l} u_1 = 0 \\ u_2 = 0 \end{array} \right\}, \text{ where } \left\{ \begin{array}{l} u_1 = F_x \\ u_2 = T_\gamma \end{array} \right\}$$

According to these equilibrium points the system matrix (A), and the input matrix (B), are found to be:

$$A = \begin{bmatrix} 0 & 0 & 0 & 0 & 1 & 0 & 0 & 0 \\ 0 & 0 & 0 & 0 & 0 & 1 & 0 & 0 \\ 0 & 0 & 0 & 0 & 0 & 0 & 1 & 0 \\ 0 & 0 & 0 & 0 & 0 & 0 & 0 & 1 \\ -101.496 & 0 & 0 & 0 & 0 & 0 & 0 & 0 \\ 0 & -117.72 & 0 & 0 & 10 & 0 & 0 & 0 \\ 0 & -49.05 & 0 & 0 & 5 & 0 & 0 & 0 \\ 13.646 & 0 & 0 & 0 & 0 & 0 & 0 & 0 \end{bmatrix} \quad (2.32)$$

$$B = \begin{bmatrix} 0 & 0 \\ 0 & 0 \\ 0 & 0 \\ 0 & 0 \\ 0 & -0.0093 \\ 0.0333 & 0 \\ 0.0167 & 0 \\ 0 & 0.0015 \end{bmatrix} \quad (2.33)$$

Now the system and the input matrices are obtained; so from these matrices, and those of the output, which are matrices C, and D, we can get the transfer functions of the system depending on the considered states to be the outputs.

### 2.3.3 Transfer Functions of the Jib Crane System

As mentioned before, there are three input motors, which are rotation, translation, and hoisting, but two inputs are considered in the modeling, which are the rotation, and translation. In this system, all states can be considered as outputs, or at least the states that represent the displacements which are in-of-plane, out-of-plane, translational, and rotational displacements, so we can get the transfer functions

between the inputs and these outputs. However there are two physical outputs that are interested in the system, which are the translational displacement represented in state  $x_3$ , and rotational velocity represented in state  $x_8$  so these outputs:

$$\begin{aligned} y_1 &= x_3 \\ y_2 &= x_4 \end{aligned} \tag{2.34}$$

Accordingly there are two output matrices, which they are:

$$C = \begin{bmatrix} 0 & 0 & 1 & 0 & 0 & 0 & 0 & 0 \\ 0 & 0 & 0 & 1 & 0 & 0 & 0 & 0 \end{bmatrix} \tag{2.35}$$

Since the outputs are just the translational displacement, and rotational speed, the feed-forward matrix (matrix D) is zero for the both outputs.

Now the state space model for the system can be written by substitution the matrices A, B, C, and D in Equation (2.20).

$$\begin{aligned} \dot{x} &= Ax + Bu \\ y &= Cx + Du \end{aligned} \tag{2.36}$$

According to these two state space models (considering two output matrices), we can get the transfer functions in this system, using the following Equation:

$$G(s) = \frac{Y(s)}{U(s)} = C(sI - A)^{-1}B + D \tag{2.37}$$

According to the dimensions of the matrix A which is  $8 \times 8$ , and that of C, which is  $1 \times 8$ , and of B, which is  $8 \times 2$ ; it can be found that the output transfer

functions will be four, which they are shown in Equations (2.38), (2.39), (2.40), and (2.41).

$$G_1(s) = \frac{X(s)}{F(s)} = \frac{0.01667 s^2 + 0.327}{s^4 + 117.7 s^2} \quad (2.38)$$

$$G_2(s) = \frac{X(s)}{T_y(s)} = \frac{-0.04637 s^3 - 0.9097 s}{s^6 + 219.2 s^4 + 1.195e004 s^2} \quad (2.39)$$

$$G_3(s) = \frac{\gamma(s)}{T_y(s)} = \frac{0.001546 s^2 + 0.03032}{s^3 + 101.5 s} \quad (2.40)$$

$$G_4(s) = \frac{\gamma(s)}{F(s)} = 0 \quad (2.41)$$

Where:

- $G_1(s)$ : is the transfer function between the input from the motor of translation, and the linear displacement output.
- $G_2(s)$ : is the transfer function between the input from the motor of rotation, and the linear displacement output.
- $G_3(s)$ : is the transfer function between the input from the motor of rotation, and the rotational speed output.
- $G_4(s)$ : is the transfer function between the input from the motor of translation, and the rotational speed output, and it is zero, this is logic because there is no effect from the motor of translational motion on the rotational speed.

In order to have an idea about the effect of the rotational speed, and the trolley position as inputs, on the in-of-plane, and out-of-plane angles as outputs which are

$\phi(t)$  and  $\theta(t)$  respectively, the transfer functions that relates these outputs to those inputs must found. The output matrices will be:

$$C = \begin{bmatrix} 1 & 0 & 0 & 0 & 0 & 0 & 0 & 0 \\ 0 & 1 & 0 & 0 & 0 & 0 & 0 & 0 \end{bmatrix} \quad (2.42)$$

And as previously mentioned; D matrix is zero, and depending on the dimensions of the matrices, A, B, and C, there will be four transfer functions. So using Equation (2.37) these transfer functions will be:

$$G_1(s) = \frac{\theta(s)}{F(s)} = 0 \quad (2.43)$$

$$G_2(s) = \frac{\theta(s)}{T_\gamma(s)} = \frac{-0.009274}{s^2 + 101.5} \quad (2.44)$$

$$G_3(s) = \frac{\phi(s)}{F(s)} = \frac{0.03333}{s^2 + 117.7} \quad (2.45)$$

$$G_4(s) = \frac{\phi(s)}{T_\gamma(s)} = \frac{-0.09274 s}{s^4 + 219.2 s^2 + 1.195e004} \quad (2.46)$$

As shown in Equations (2.43), through to (2.44), the input from the motor of translational motion don't affect the out-of-plane angle, it just affect on the in-of-plane angle, whereas the input from the motor of rotational motion affects both of them, and this agrees with our consideration, that is the control of the rotational motion motor can be enough to decrease these angles, if and only if a discrete motions is applied to the system.

## **2.4 Lifting Force**

### **2.4.1 Introduction Electromagnet**

The simplest type of electromagnet is a coiled piece of wire. A coil forming the shape of a straight tube is called a solenoid; a solenoid that is bent so that the ends meet is a toroid. Much stronger magnetic fields can be produced if a core of paramagnetic or ferromagnetic material (commonly soft iron) is placed inside the coil. The core concentrates the magnetic field that can then be much stronger than that of the coil itself.

Current ( $I$ ) flowing through a wire produces a magnetic field ( $B$ ) around the wire. The field is oriented according to the left-hand rule (Faraday's second law).

Magnetic fields caused by coils of wire follow a form of the right-hand rule (for conventional current or left hand rule for electron current). If the fingers of the left hand are curled in the direction of electron current flow through the coil, the thumb points in the direction of the field inside the coil. The side of the magnet that the field lines emerge from is defined to be the north pole.

### **2.4.2 Electromagnets and permanent magnets**

The main advantage of an electromagnet over a permanent magnet is that the magnetic field can be rapidly manipulated over a wide range by controlling the amount of electric current. However, a continuous supply of electrical energy is required to maintain the field.



As a current is passed through the coil, small magnetic regions within the material, called magnetic domains, align with the applied field, causing the magnetic field strength to increase. As the current is increased, all of the domains eventually become aligned, a condition called saturation. Once the core becomes saturated, a further increase in the current will only cause a relatively minor increase in the magnetic field. In some materials, some of the domains may realign themselves. In this case, part of the original magnetic field will persist even after power is removed, causing the core to behave as a permanent magnet. This phenomenon, called remnant magnetism, is due to the hysteresis of the material.

### 2.4.3 Magnetic force analysis

In lifting, we will use a magnetic force, which can hold a ferromagnetic materials such as steels (figure 2.5). Computing the force on ferromagnetic materials is, in general, quite complex. This is due to fringing field lines and complex geometries. It can be simulated using finite element analysis. However, it is possible to estimate the maximum force under specific conditions. If the magnetic field is confined within a high permeability material, such as certain steel alloys, the maximum force is given by:

$$F = \frac{B^2 A}{2\mu_0} \quad (2.47)$$

Where:

F : is the force in newtons

B: is the magnetic field in teslas

A : is the area of the pole faces in square meters

Laser position sensors send out a narrow pulse of light and determine the distance to the reflecting object by measuring the time for the pulse to return. The motion of the trolley is thus not interfered with. The measured object must reflect light. Laser sensors are also robust, but at a high price, they are judged too expensive.[6]

Finally, the ultrasonic sensor (figure(3.8)) is similar to its laser counterpart, except it sends out a sound wave instead of a light wave. Like the laser sensor, an ultrasonic sensor does not interfere with the motion of the measured object. Two possible problems exist in the area of robustness. The first deals with the variation in the speed of sound. In contrast to light, sound needs a medium to travel in and the speed of propagation varies with the medium's (air's) temperature. This potential problem is solved by selecting an ultrasonic sensor with temperature compensation. The second potential problem is that air forced through a nozzle creates a whistling sound with harmonics in the ultrasonic range. This could be a problem with the prevalence of pneumatic devices, such as hoists, in material handling environments. The effect is minimized by selecting an ultrasonic sensor which emits a high frequency (low wavelength) sound wave. Thus the two uncertainties in the area of robustness can be dealt with and the ultrasonic sensor is chosen to measure the trolley's radial position.

Ultrasonic sensors emit an ultrasound beam of conical pattern, a larger beam angle would produce a conical pattern which could include other objects, particularly, the boom. If any of these objects includes a surface, even a small nick, perpendicular to the sound wave, it is the distance to this false target which will be measured.

$\mu_0$  :is the permeability of free space

In the case of free space (air),  $\mu_0=4\pi*10^{-7}\text{H.m}^{-1}$ . In a closed magnetic circuit:

$$B = \frac{\mu_0 NI}{L} \quad (2.48)$$

Where:

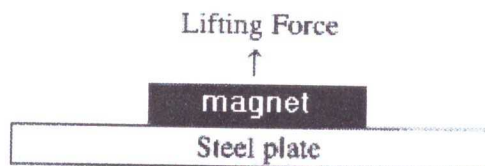
$N$  :is the number of turns of wire around the electromagnet

$I$  :is the current in amperes

$L$  :is the length of the magnetic circuit

Substituting the above in equation (2.47) ,

$$F = \frac{\mu^2 N^2 I^2 A}{2\mu_0 L^2} \quad (2.49)$$



**Figure(2.5):**Magnetic lifting force.

The magnetic flux density would be one third of the maximum flux density by the magnet because of the air gap between the magnet and the part before lifting starts. On the other hand, the magnetic force must be bigger than the weight of the part (9.8 N), so we set the magnetic force to be 12 N. many parameters in equation(2.49) could be change to get the needed force, we will fix the dimensions

and the turns number of the magnet coil, so we can get the needed force by calculating the current needed to generate a sufficient force.

## **2.5 statics and mechanical analysis**

The conveyor was designed for 860 n/m , and we will load it by 51.6 n/m(equation (2.9)) so we have a big factor of safety in our use of the conveyor. Besides, the crane designed to hoist four kilograms , and we will use it hoist less than two kilograms, since the mass of the part is one kilogram and the mass of the magnet less than one kilogram. So the two systems can handle our use, and we don't need to analyze the stresses and deformation in the two systems because we are in the safe side.

## **Chapter Three**

### **Actuators and Sensors**

#### **3.1 Introduction**

In this chapter we will introduce the actuators and sensors which will be used in the project. Four actuators are needed, one for the conveyor to detect the part, and the others for the jib crane, one for rotational motion, the second for translational motion and the third for hoisting. All actuators are DC motors since DC motors are easy to control. The selection of the motors depends on the needed torques, these will be calculated in this chapter.

In this project we need at least four sensors, three of them to determine the position of the crane, the fourth is to give a signal if there is a part or not on the desired location on the conveyor, sensors specifications will be presented in this chapter.

#### **3.2 Motors Selection**

In this chapter the needed torque of each motor will be calculated, according to this torque the motor will be selected

### 3.2.1 Motor of the conveyor

To select the motor needed to drive the conveyor, the needed torque must be calculated. We know that the force which will move the part is friction force between the part and the belt (figure (3.1)), so the total force needed to drive the belt is the number of parts multiplied by the force on each part, neglecting the friction between the belt and the slider.

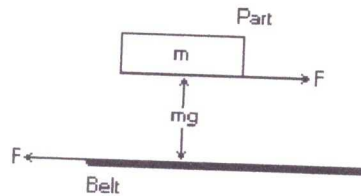


**Figure 3.1:** Force on the part.

From equation(2.1.a), setting the acceleration to be  $0.1 \text{ m/s}^2$  and neglecting the mass of the belt we get

$$F = m_{total} * \ddot{x} + F_{sb} \quad (3.1)$$

We know that  $m_{parts}=n.m$ ,  $F_{sb}$  is friction between the belt and the slider. This friction is negligible, the belt mass is too small relative to the parts mass and the rollers are frictionless, so

$$F = (n.m)\ddot{x} = (5 * 1 * 1) = 5 \text{ N} \quad (3.2)$$

So the torque of the motor is

$$T = F_T * r \quad (3.3)$$

Where  $r$  is the radius of the drive roll which is 5cm so the needed torque to drive the conveyor is

$$T = 5 * 0.05 = 0.25 \text{ N.m} \quad (3.4)$$

To calculate the output power of this motor as the following equation

$$P = T \cdot \omega \quad (3.5)$$

The load will reach the final position at speed of (0.42 m/s), and the radius of the shaft that drive the belt of conveyor is (0.05 m), so we can calculate the angular velocity of this motor by the following equation

$$\omega = \frac{V}{r} = \frac{0.42}{0.05} = 8.4 \text{ radian/sec} \quad (3.6)$$

By substituting in equation(3.3), we obtain

$$P = 0.25 * 8.4 = 2.1 \text{ watt} \quad (3.7)$$

From data sheet of worm gear that will use for transmit the power from motor to the load, the efficiency of this gear is 85%, then the output power of the DC motor will be

$$P = 0.25 / 0.85 = 2.47 \text{ Watt} \quad (3.8)$$

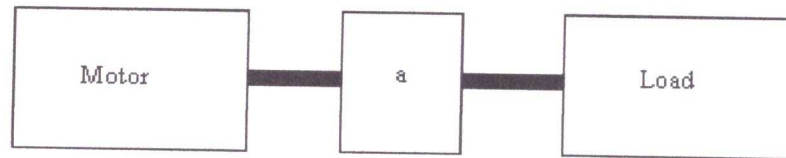
### 3.2.2 Motor for rotational motion of the crane

The needed torque for the rotational motion must override the moving part load and the friction forces produced on the rotary joint. But the used bearing on the joint has a very small coefficient of friction which produces a small friction forces compared with load so these forces can be neglected.

The needed torque is given by the equation

$$T = J_e \alpha \quad (3.9)$$

Where  $J_e$  is the equivalent moment of inertia of the moving parts reflected to the motor joint, and  $\alpha$  is the angular acceleration. The motor shaft is connected to the load throughout a sprocket and chain with a transmission ratio (a) (figure(3.2)).



**Figure(3.2):** Load motor connection.

The driven sprocket 78 teeth and the driver has 19, so the transmission ratio is about 0.25. The equivalent moment of inertia is given by

$$J_e = a^2(J_{sprocket} + J_{upper\ flange} + J_{boom\ mount} + J_{boom} + J_{trolley} + J_{load}) \quad (3.10)$$

These moments of inertia were found by CATIA as shown in table (3.1)

**Table (3.1):**inertias of rotating parts.

Part	Inertia (kg.m <sup>2</sup> )
Sprocket	0.02
Upper flange	0.003
Boom mount	0.009
Boom	0.518
Trolley	0.062
Load	0.003
Total inertia	0.615



Substituting the values of the moments of inertia in equation (3.10) we get

$$J_e = 0.25^2(0.615) = 0.0384 \text{ Kg. m}^2 \quad (3.11)$$

if we set the angular acceleration to be  $1 \text{ rad/s}^2$  the torque will be (equation (3.9))

$$T = (0.0384)(1) = 0.0384 \text{ N.m} \quad (3.12)$$

The previous students used a three phase AC induction motor, we will replace it with a sufficient DC motor, dc motors advantages are generally the reason for its choice, which are; Firstly the excellent speed control with very good torque and horsepower characteristics because its armature design and function ,it has very smooth torque from zero rpm to base speed .the dc motor also has full-rated horsepower above base speed. So a motor with 60 rpm rated speed and 14 V input will supply the needed torque.

### **3.2.3 Translational Motion Motor**

The motion of the trolley is achieved using a power screw, the trolley has 4 rollers to move along the boom, and a hanger to connect the trolley's nut to the power screw as shown in figure (3.3).

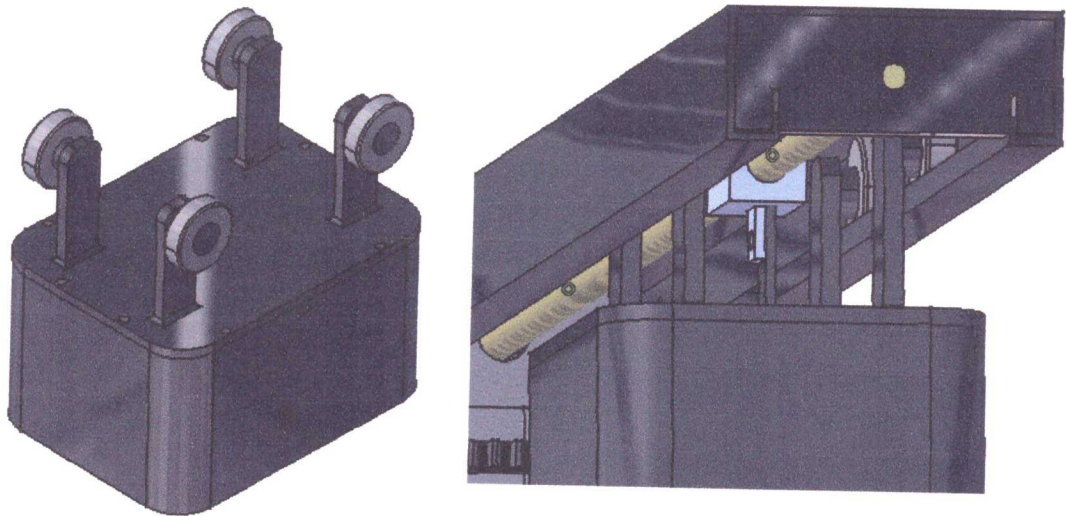


**figure (3.3):** Motion of the trolley.

The force produced by the motor must override the friction between the screw and the trolley's nut, since the number of meshed teeth are 33, the friction force will be

$$F_{friction} = 33N\mu_s \quad (3.13)$$

Where  $N$  is the normal force, in this case the load on the hanger and wheels is distributed equally. Each support has 2 kg since the weight of these parts and load is 10 kg. On the other hand ( $\mu_s$ ) the static coefficient of friction between the materials which are steels is 0.18. so the friction force is

$$F_{friction} = 33 * 2 * 9.8 * 0.18 = 116.54 \text{ N} \quad (3.14)$$

Now the needed torque to drive the trolley can be found as

$$T = F_{friction} * r = 116.54 * 0.008 = 0.932 \text{ N.m} \quad (3.15)$$

Where  $r$  is the radius of the power screw (8 mm). A sufficient motor selected by the students who worked on this project with 60 rpm rated speed and 14 V input, and this motor will not be changed.

### 3.2.4 Hoisting Motor

The hoisting is achieved using a motor with a pulley on its shaft and a cable, the needed torque must generate a tension force in the cable bigger than the lifted weight, the mass of the load is less than 2 Kg , so a force of 20 N can do the job. The radius of the pulley is 0.01 m so the needed torque is

$$T = Fr = 20 * 0.01 = 0.2 \text{ N.m} \quad (3.16)$$

A suitable DC motor is used to that job with 60 rpm rated speed and 14V input voltage, and this motor will not be changed.

### 3.3 Sensors

Sensors are very important in our project because they will give signals, those signals give information about the system. The minimum number of sensors needed is four sensors, each sensors will be described in this section.

#### 3.3.1 Part Detecting Sensor

To determine the existence of the part in the desired position on the conveyor, an inductive proximity sensor (figure(3.4)) will be used, which gives a signal if a part is in the desired position.

An inductive proximity sensor is one of a class of sensors, called proximity sensors, which detects objects without actually touching with them. Photoelectric sensors and capacitive proximity sensors are also found in this category. The inductive proximity sensor only detects metallic objects and ignores all others, and has many uses which capitalize on this feature.

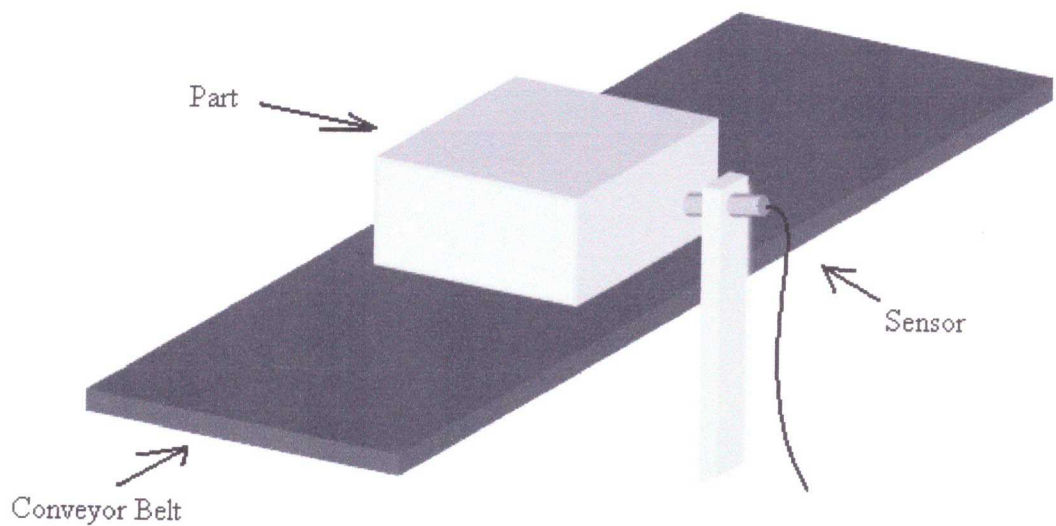


**Figure(3.4):**Inductive proximity sensor.

The inductive sensor is a simple enough device at the fundamental level. It is simply a coil of wire with a current passing through it. It completely ignores most objects which pass near this coil. However, when a metallic object passes near it, it acts as a core material in the inductive loop which increases its inductance significantly. Most non-metallic objects have a negligible effect on its inductance. The complex part of the sensor is the sensing circuitry which detects this change in inductance by monitoring the electric current in the loop. When the inductance changes enough, it triggers the sensor's output, which sends a signal to some other machine to do whatever it is, it is supposed to do when a metallic object is near the sensor. [5]

Some important properties must be considered, such as the sensing distance required which is the distance between the tip of the sensor and the object to be

sensed. Other important feature is the output type, is it digital or analog. Besides , the environment on which the sensor will be placed such as the temperature and or under water working. The type of mounting is also important is it flush or not. The most important feature in our consideration is the output type, the others can be deal with, we need a sensor to give a digital signal (on-off) if there is a part or not. The sensor mounting shown in figure (3.5).

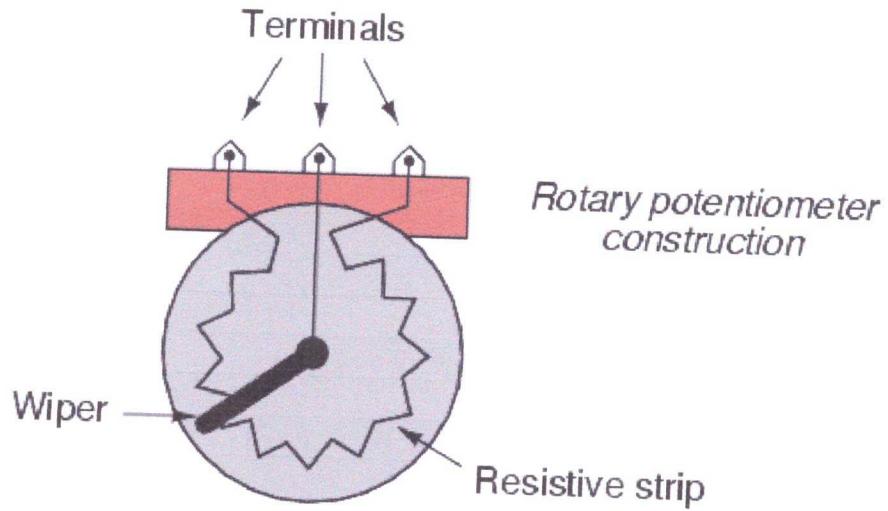


**Figure(3.5):** Sensor mounting.

### 3.3.2 Angle of Rotation Sensing

To sense the angle of the boom a potentiometer is used, potentiometers measure the angular position of a shaft using a variable resistor. A potentiometer is shown in Figure (3.6). The potentiometer is resistor, normally made with a resistive strip. A wiper moves along the surface of the resistive strip. As the wiper moves toward one end there will be a change in resistance proportional to the distance

moved. If a voltage is applied across the resistor, the voltage at the wiper interpolates the voltages at the ends of the resistor.



Figure(3.6): Potentiometer.

The potentiometer in Figure 3-6 is being used as a voltage divider. As the wiper rotates the output voltage will be proportional to the angle of rotation.

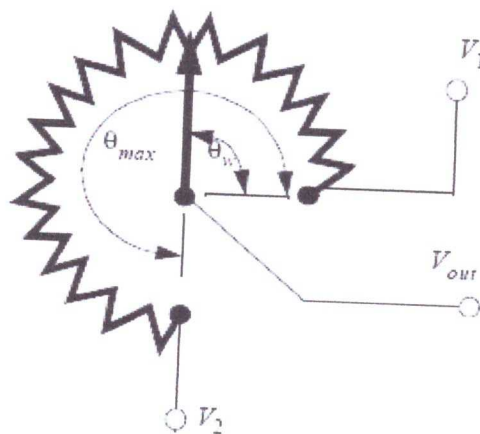


Figure (3.7): Potentiometer as a Voltage Divider.

$$V_{out} = (V_2 - V_1) \left( \frac{\theta_w}{\theta_{max}} \right) + V_1 \quad (3.17)$$

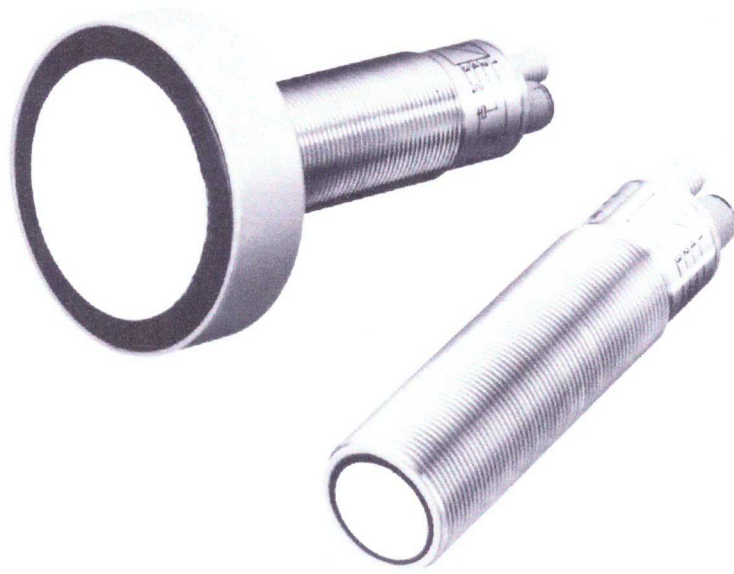
Potentiometers are popular because they are inexpensive, and don't require special signal conditioners. But, they have limited accuracy, normally in the range of 1% and they are subject to mechanical wear.

Potentiometers measure absolute position, and they are calibrated by rotating them in their mounting brackets, and then tightening them in place. The range of rotation is normally limited to less than 360 degrees or multiples of 360 degrees. Some potentiometers can rotate without limits, and the wiper will jump from one end of the resistor to the other.

### 3.3.3 Trolley Radial Distance Sensing

The desired attributes of the radial position sensor are lack of interference with the trolley's motion, low cost, robustness and accurate. Three types of position sensors are considered: reeled cord, laser, and ultrasonic.

A reeled cord position sensor physically attaches a cord to the device being measured. The device is both inexpensive and robust. However, like on a tape measure, a retractile force is necessary to draw the cord back into the reel. Thus, this type of sensor applies a force, which generally increases with measured distance, to the measured object. Because of the very low rolling friction in the radial direction, this type of sensor is deemed unacceptable. [6]



**Figure(3.8):** Ultrasonic Sensors.

When selecting a sensor, some properties must be determined such that: the range of distance to be measured, the output type and range and the angle of the beam. The environmental conditions must be also considered. The needed output is analog(i.e:0-10V) and the range of distance up to 1m. A suitable sensor for this job is a Honeywell ultrasound sensor 946 series, which has a supply voltage of (10-30V) and analog output of (0-10V) , this sensor has a linearity error less than 0.1% and repeatability less than 0.1% of reading, the distance range up to 6000 mm.

The mounting of the sensor is below the boom adverse to the trolley as shown in figure(3.9). The distance of the sensor below the boom limited by the angle of the





**Figure(3.9):** Sensor mounting and conical beam.

ultrasound beam, as the max distance to be measured is about 0.9 m and the angle of the beam is  $5^\circ$ , we can calculate the minimum distance under the boom at which the sensor can be mounted(figure(3.10)) as

$$L = Distance_{max} * \tan\left(\frac{Beam\ angle}{2}\right) = 90 * \tan\frac{5}{2} = 4\ cm \quad (3.18)$$

Hence, the ultrasonic sensor must place more than 4 cm under the boom.

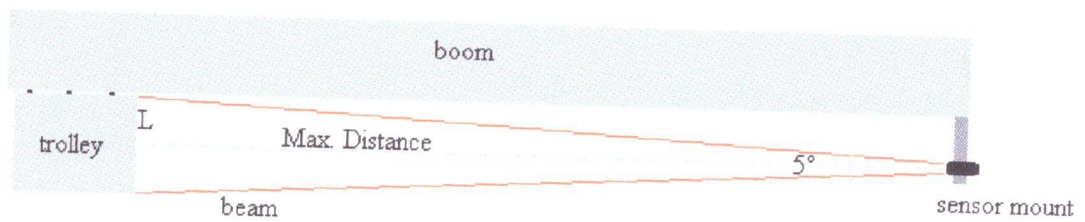


**Figure (3.10):** Detailed sensor mounting.

### 3.3.4 Hoisting Distance Sensing

Hoisting distance sensing can be performed using two types of sensors used to measure the trolley radial distance are considered: rotational optical encoder, ultrasonic sensor.

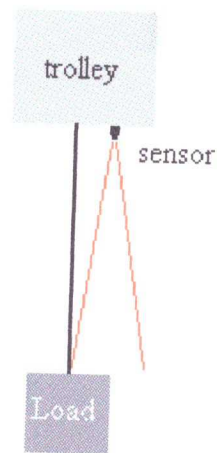
The hoisting distance is very important for lifting and lowering the part, since that we should use the rotational optical encoder that often measures using pulse counting methods, optical position transducer are becoming popular for the following reasons:

- They are inherently digital.
- They immune from electrical interference.
- No mechanical connection to the sensing element is made.
- Simplicity, reliability, accuracy, and suitability for sensitive applications.

Optical encoder is a circular device in the form of a disk on which a digital pattern is etched. The inscribed pattern is sensed by means of a sensing head. The rotary disk is normally coupled to a shaft. As the shaft rotates, a different pattern is

generated for each resolvable position. Optical encoder sensors are also robust, but at a high price, they are judged too expensive. [8]

In this case, hoisting distance sensing can be performed using the type of sensors used to measure the trolley radial distance, in this case the sensor must be mounted on the trolley adverse to the load as shown in figure (3.11).



**Figure(3.11):** Sensor mounting to measure hoisting distance.

## **Chapter Four**

### **Interfacing System**

#### **4.1 Introduction**

In this chapter Interfacing between the computer and the sensors/actuators will be explained, which includes the data acquisition card, isolation circuits, driving circuits...etc. On the other hand Real time windows target in MATLAB will be explained as well.

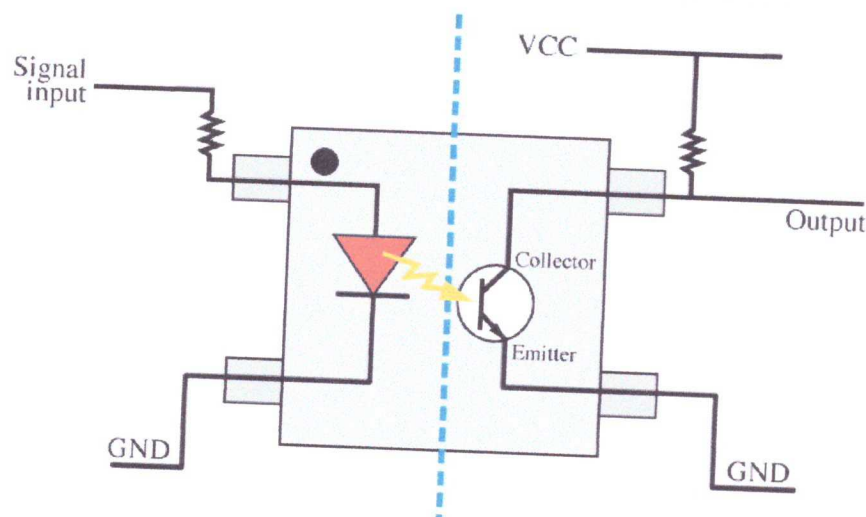
#### **4.2 Interfacing**

##### **4.2.1 Digital Isolation(Optocouplers)**

There are many situations where signals and data need to be transferred from one subsystem to another within a piece of electronics equipment, or from one piece of equipment to another, without making a direct electrical connection. Often this is because the source and destination are (or may be at times) at very different voltage levels, like a microprocessor which is operating from 5V DC but being used to control a triac which is switching 240V AC. In such situations the link between the two must be an isolated one, to protect the microprocessor from overvoltage damage.

Relays can of course provide this kind of isolation, but even small relays tend to be fairly bulky compared with ICs and many of today's other miniature circuit components. Because they're electro-mechanical, relays are also not as reliable and only capable of relatively low speed operation. Where small size, higher speed and greater reliability are important, a much better alternative is to use an optocoupler. These use a beam of light to transmit the signals or data across an electrical barrier, and achieve excellent isolation.

Optocouplers typically come in a small IC package, but are essentially a combination of two distinct devices: an optical transmitter, typically a gallium arsenide LED (light-emitting diode) and an optical receiver such as a phototransistor or light-triggered diac. The two are separated by a transparent barrier which blocks any electrical current flow between the two, but does allow the passage of light. The basic idea is shown in figure(4.1), along with the usual circuit symbol for an optocoupler.

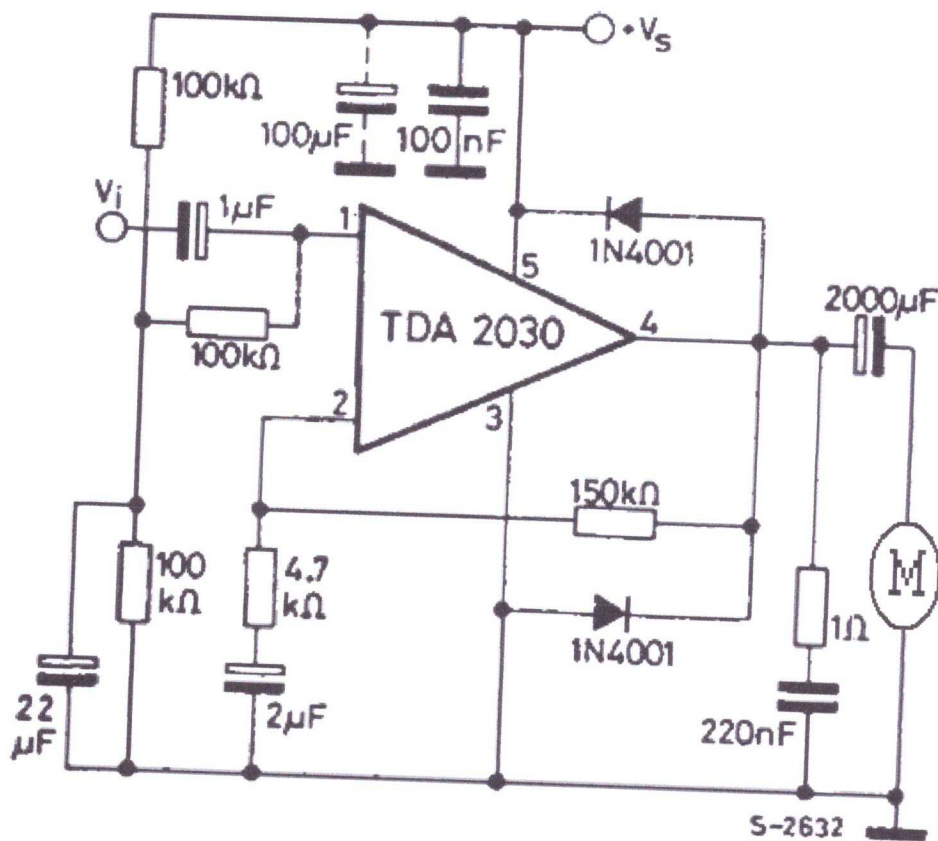


**Figure(4.1):** An optocoupler

In this project optocouplers will be used to isolate the DAC from the input and output digital signals such as the proximity sensor signal.

#### 4.2.2 Rotational Motor interfacing

The DC motor used in rotational motion needs high current relative to the output current from the DAC, so a power amplifier must be placed between the DAC and the motor to drive the motor. An audio power amplifier (TDA2030) can take the charge. This circuit (figure 4.2) called the driving circuit which gives an efficient current to drive the motor according to the signal from the DAC.

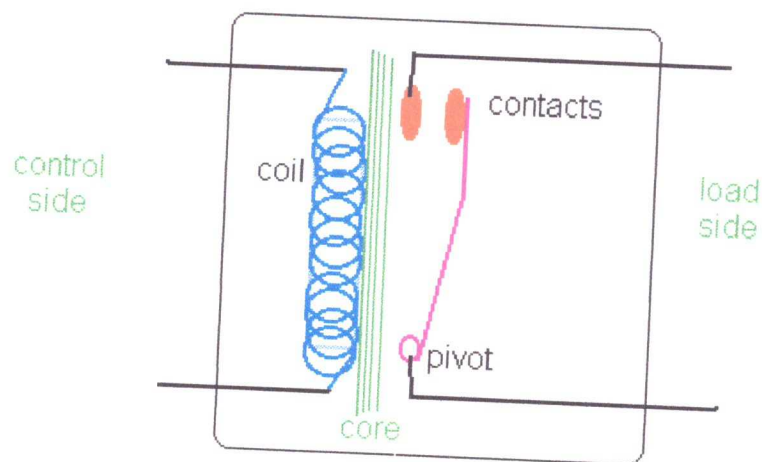


Figure(4.2): Driving Circuit

### 4.2.3 Electrical Switches(Relayas)

A relay is an electrical switch that opens and closes under the control of another electrical circuit. Because a relay is able to control an output circuit of higher power than the input circuit, it can be considered to be, in a broad sense, a form of an electrical amplifier.

When a current flows through the coil, the resulting magnetic field attracts an armature that is mechanically linked to a moving contact. The movement either makes or breaks a connection with a fixed contact. When the current to the coil is switched off, the armature is returned by a force approximately half as strong as the magnetic force to its relaxed position. Usually this is a spring, but gravity is also used commonly in industrial motor starters. Most relays are manufactured to operate



**Figure(4.3):** relay principle

quickly. In a low voltage application, this is to reduce noise. In a high voltage or high current application, this is to reduce arcing.

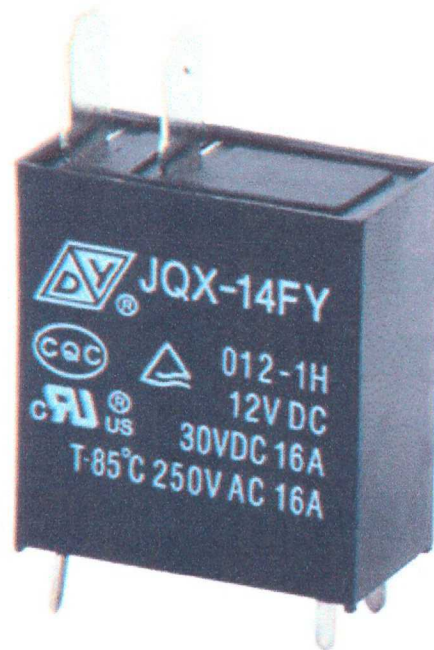


Figure (4.4): solid state relay

A solid state relays are used in this project. A solid state relay (SSR) is a solid state electronic component that provides a similar function to an electromechanical relay but does not have any moving components, increasing long-term reliability. With early SSR's, the tradeoff came from the fact that every transistor has a small voltage drop across it. This collective voltage drop limited the amount of current a given SSR could handle. These relays are used to control the conveyor motor and the magnet coil (on-off control).

### 4.3 Data Acquisition Card

A **data acquisition card** is a basic A/D converter coupled with an interface that allows a personal computer to control the actions of the A/D, as well as to capture the digital output information from a conversion. A data acquisition card

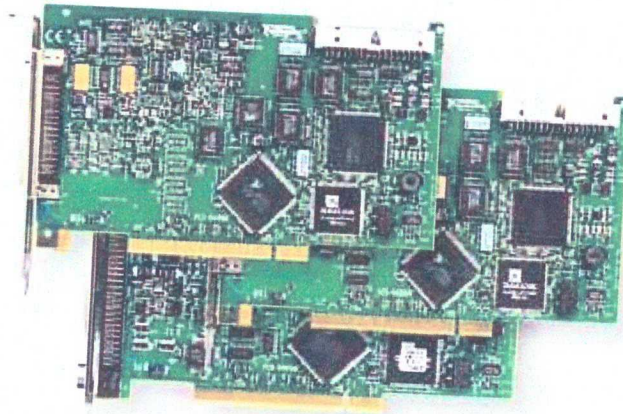


plugs directly into a personal computer's bus. All the power required for the A/D converter and associated interface components on the data acquisition card is obtained directly from the PC bus.

Today, a data acquisition card is more than a simple A/D function on a board. A data acquisition card can offer measurements of up to 64 channels at a resolution of 16 bits, (one part in 65,536) with data throughput rates up to 20 million samples per second. A data acquisition card can and often does include discrete digital bi-directional I/O lines, counter timers, and D/A converters for outputting analog signals for control applications.

An NI PCI-6024E DAC (figure (4.5)) from National Instruments is used in this project. National Instruments is one of the largest companies that provide electrical solutions. It is famous for providing data acquisition cards. Data acquisition cards are those cards that are used as interfaces between a plant and a computer in order to control the plant in real time environment. In the project the PCI-6024E DAC card was used. The 6024E features 16 channels of analog input, two channels of analog output, a 68-pin connector and eight lines of digital I/O. The PCI-6024E DAC card uses the National Instruments DAC-STC system timing controller for time-related functions. The DAC-STC consists of three timing groups that control analog input, analog output, and general-purpose counter/timer functions. The three groups include a total of seven 24-bit and three 16-bit counters and a maximum timing resolution of 50 ns. The DAC-STC makes possible such applications as buffered pulse generation, equivalent time sampling, and seamless changing of the sampling rate. In many DAC systems, it is not easy to synchronize several measurement functions to a common trigger or timing event. Such devices have the Real-Time System Integration (RTSI) bus to solve this problem. In the PCI-6024E DAC card, the RTSI bus consists of the National Instruments RTSI bus

interface and a ribbon cable to route timing and trigger signals between several functions on as many as five DAC devices in a computer.



**Figure(4.5):** PCI-6024E DAQ card

In order to use the PCI-6024E DAC card, it is required to have MATLAB 6.5 or later or Simulink 5.0 or later with Real Time Windows Target 1.0 or later, PCI interface and NI-DAC 7.x drivers.

#### **4.4 Real Time Windows Target in MATLAB**

The Real-Time Windows Target has many features. An introduction to these features and the Real-Time Windows Target software environment will help in developing a model for working with Real-Time Windows Target.

Counter Input, and Encoder Input blocks call the drivers for input and output. A driver block use values equal to voltage could be choose, normalize values from 0 to +1, normalize values from -1 to +1, or used the raw integer values from the A/D or D/A conversion press. Communication between Simulink and the real-time application is through the Simulink external mode interface module. This module talks directly to the real-time kernel, and is used to start the real-time application, change parameters, and retrieve scope data.

The real-time application runs in real time on the PC and has a compiled code, a relation to Simulink model, a relation to the kernel and a check sum. The compiled code is created from the generated C code using a Microsoft Visual C/C++ compiler. The executable code contains a binary form of all Simulink model components, connections between blocks, time dependencies, and variables in the Simulink blocks. The executable code must be loaded and executed directly by the Real-Time Windows Target kernel. The Simulink model and the executable contain a checksum value. The kernel uses this checksum value to determine if the Simulink model structure, at the time of code generation, is consistent with the real-time application structure during execution.

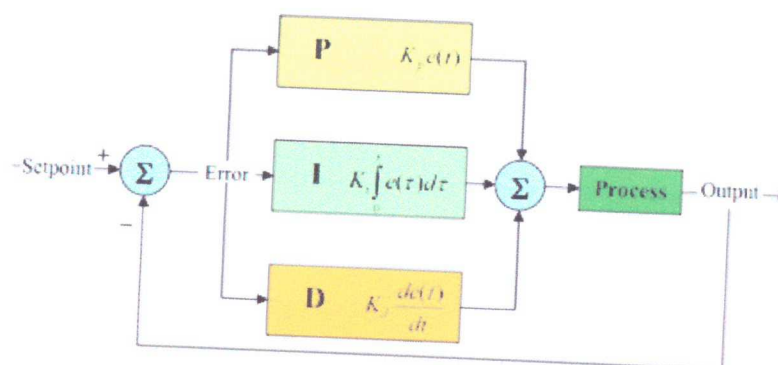
In order to use the Real Time Windows Target, the I/O board drivers must be compatible with it. NI-DAQ 7.x drivers are compatible with the RTWT. The model must be designed, built, and tested in non real time mode before being executed in the real time mode. The procedures for the non real time simulation are similar to the procedures for simulating a model in Simulink in the normal mode. For the real time simulation model, please refer to Appendix B.

## 5.2 Rotational Motor Control

### 5.2.1 PID controller Design for Rotational-Motion Motor

A proportional–integral–derivative controller (PID controller) is a generic control loop feedback mechanism widely used in industrial control systems. A PID controller attempts to correct the error between a measured process variable and a desired setpoint by calculating and then outputting a corrective action that can adjust the process accordingly.

The PID controller calculation involves three separate parameters; the Proportional, the Integral and Derivative values. The Proportional value determines the reaction to the current error, the Integral determines the reaction based on the sum of recent errors and the Derivative determines the reaction to the rate at which the error has been changing. The weighted sum of these three actions is used to adjust the process via a control element such as the position of a control valve or the power supply of a heating element.



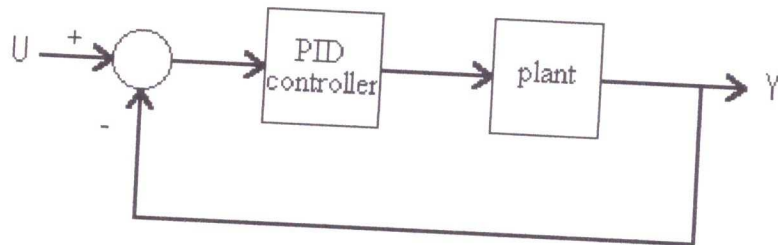
Figure(5.1): PID controller block diagram

By "tuning" the three constants in the PID controller, the PID can provide control action designed for specific process requirements. The response of the controller can be described in terms of the responsiveness of the controller to an error, the degree to which the controller overshoots the setpoint and the degree of system oscillation.

The transfer function of the PID is

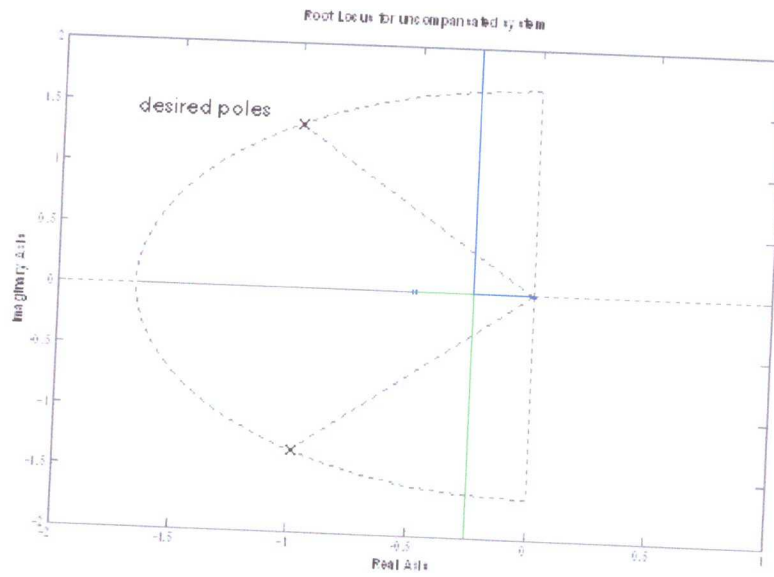
$$G_C(s) = K_P + \frac{K_I}{s} + K_D s \quad (5.1)$$

the block diagram of the plant (motor) cascaded with the controller shown in figure(5.2). Plant transfer function has been found experimentally (Appendix A).



**Figure(5.2):** block diagram of the closed loop system.

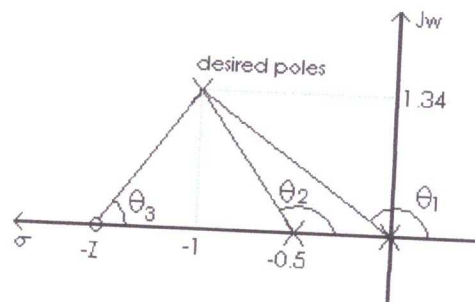
With its three-term functionality offering treatment of both transient and steady-state responses, proportional-integral-derivative (PID) control provides a generic and efficient solution to real world control problems. The PD side improves the transient response and the PI improves the steady-state error. Designing a PID



**Figure(5.3):**Uncompensated system root locus.

To compute the value of the zero, the sum of angles must equal  $180(2k+1)$ . From the geometry in figure(5.4)

$$\theta_3 - \theta_2 - \theta_1 = 180^\circ(2k + 1) \quad (5.2)$$

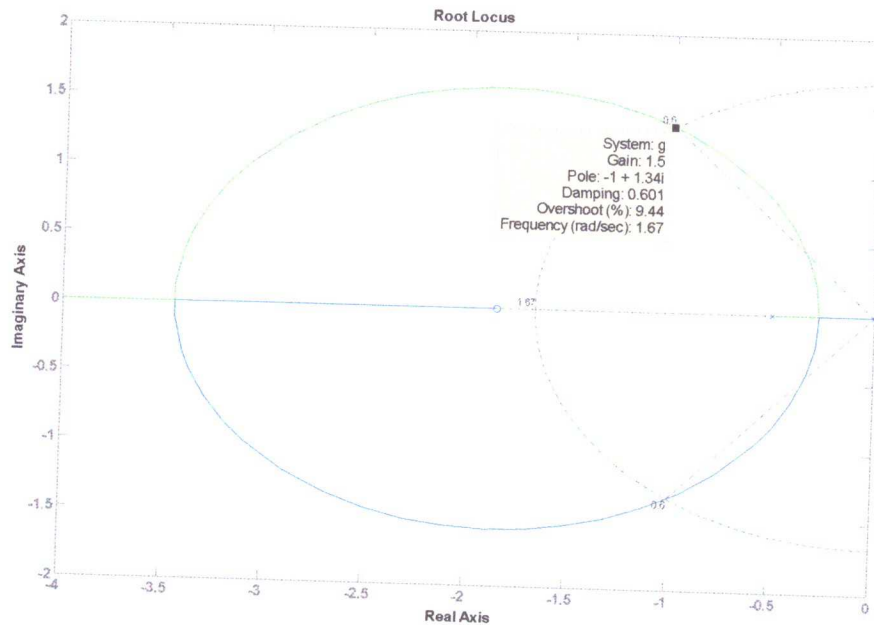


**Figure(5.4):**Calculating PD zero location.

$\theta_1 = 126.73^\circ$  and  $\theta_2 = 110.46^\circ$  so  $\theta_3 = 57.2^\circ$ , the zero location is

$$z = 1 + \frac{1.34}{\tan 57.2} = 1.86 \quad (5.3)$$

The root locus for PD-compensated system is shown in the figure(5.5).



**Figure(5.5):**PD-compensated system root locus

The transfer function of the PD controller is,  $G_{PD} = 1.5(s + 1.86)$

PI controller:

PI controller consists of a pole at origin and a zero near the origin to meet the steady-state specifications without affecting the root locus. The zero of the controller is assumed to be at  $-0.01$  and the pole at zero, so the PI controller transfer function is  $G_{PI} = \frac{s+0.01}{s}$ . The PID controller transfer function is

$$G_{PID} = G_{PD} \times G_{PI} = \frac{1.6(s+1.86)(s+0.01)}{s} \quad (5.4)$$

The root locus of the PID-compensated system is shown in figure(5.6)

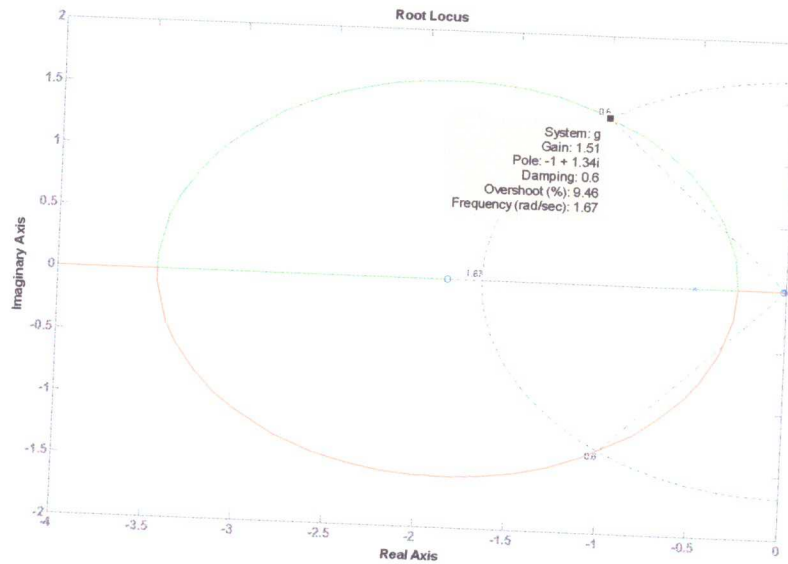
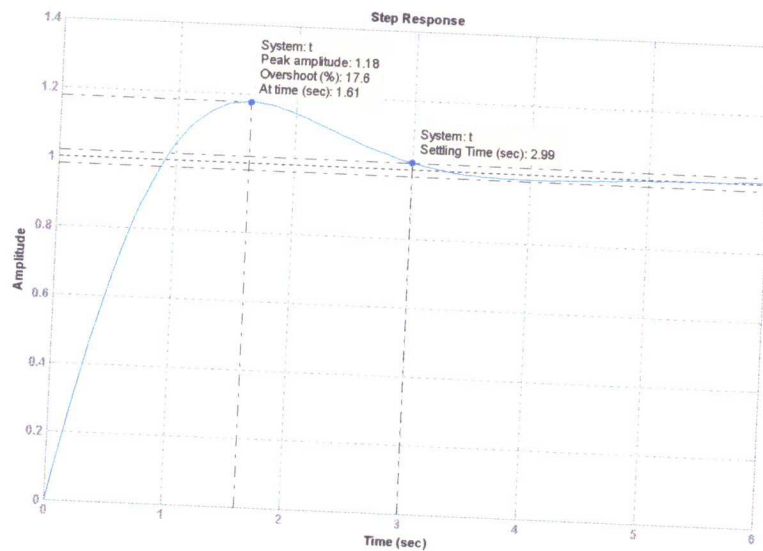


Figure (5.6):PID-compensated system root locus



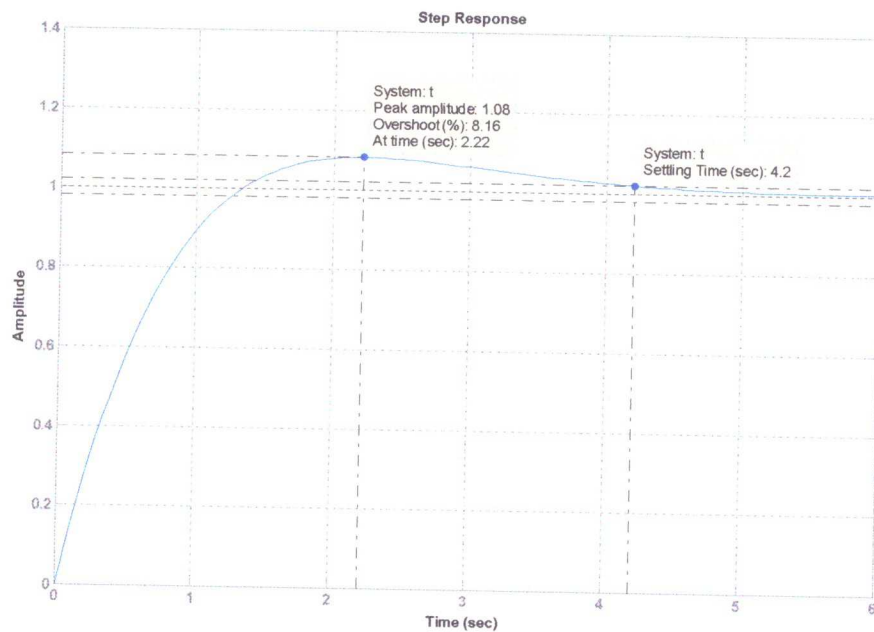
Figure(5.7):step response for PID-compensated system



We notice that the root locus of the system was not be changed the PI controller was added to the system. The response for a step input for a PID-compensated system is shown in figure(5.7).

The overshoot of the system for step input is 17.6%, but it must be less than 10%. So the PID controller parameter must be tuned to get the desired response, using SISO tool in MATLAB the desired response is gotten by changing the parameters of the PID controller, the response is shown in figure(5.8), this response corresponds to the following PID controller

$$G_{PID} = \frac{1.5(s+1)(s+0.01)}{s} \quad (5.5)$$

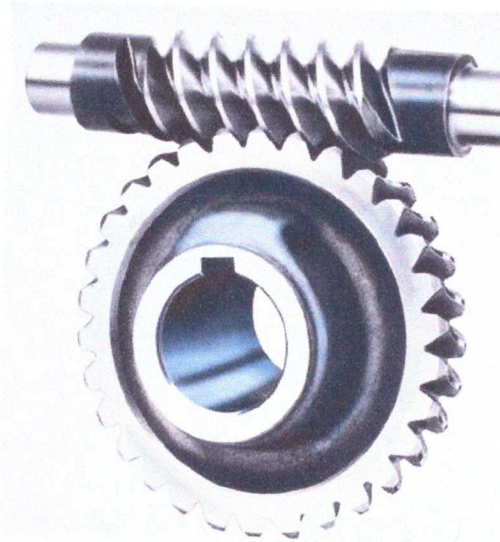


**Figure(5.8):** The desired step response

### 5.2.2 Mechanical Disturbance Rejection

Any disturbance on the system must be eliminated, this is achieved by mean of worm gear(figure(5.9)). Unlike ordinary gear trains, the direction of transmission (input shaft vs output shaft) is not reversible, due to the greater friction involved between the worm and worm-wheel, when a single start (one spiral) worm is used. This can be an advantage when it is desired to eliminate any possibility of the output driving the input. If a multistart worm (multiple spirals) then the ratio reduces accordingly and the braking effect of a worm and worm-gear may need to be discounted as the gear may be able to drive the worm.

Worm drives are a compact, efficient means of substantially decreasing speed and increasing torque. Small electric motors are generally high-speed and low-torque; the addition of a worm drive increases the range of applications that it may be suitable for, especially when the worm drive's compactness is considered.



**Figure(5.9):** Worm Gear.

An advantage of using this method is that, the disturbance rejection is achieved even though the motor is turned off.

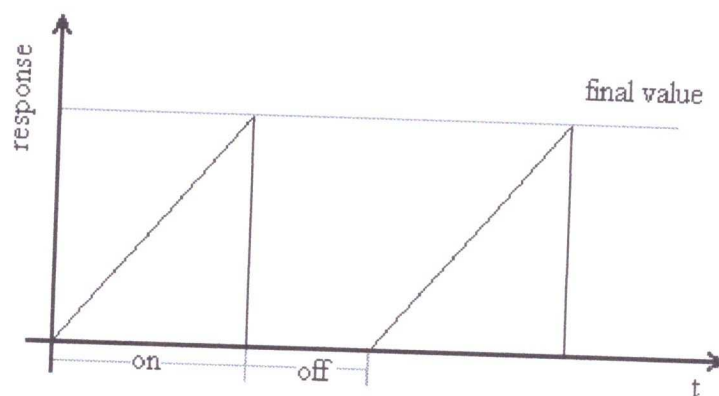
### 5.3 Conveyor Motor Control

Recalling the conveyor model (chapter2)

$$\dot{x} = \begin{bmatrix} 0 & 1 \\ 0 & 0 \end{bmatrix} \begin{bmatrix} x_1 \\ x_2 \end{bmatrix} + \begin{bmatrix} 0 \\ \frac{1}{n.m.} \end{bmatrix} F \quad (5.6)$$

$$y = \begin{bmatrix} 1 & 0 \end{bmatrix} \begin{bmatrix} x_1 \\ x_2 \end{bmatrix} \quad (5.7)$$

This system is unstable, but it will not go unstable by mean of on-off control. This model represents an open loop system which will go unstable for a step input, but the motor of the conveyor will be stopped by the proximity sensor when a part reaches it. On the other hand the friction between the belt and the slider (nonlinearities) makes the system in the stable region. A typical response for such systems shown in figure (5.10).



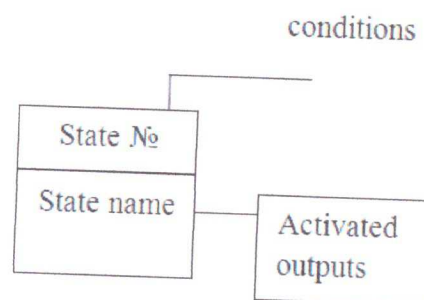
Figure(5.10): On-off control.

## 5.4 Synchronization

### 5.4.1 State Flow Method Definition

State flow method is a graphical design and development tool that helps in writing programs, it is a suitable environment for modeling logic used to control and supervise a physical plant modeled in Simulink and also in (PLC) programs.

State flow integrates with its Simulink environment to model, simulate, and analyze your system. State flow helps in designing and developing supervisory control systems in a graphical environment. It visually models and simulates complex reactive control to provide clear, concise descriptions of complex system behavior using finite state machine theory, flow diagram notations, and state-transition diagrams all in the same diagram. State flow brings system specification and design closer together. It is easy to create designs, consider various scenarios, and iterate until the State flow diagram models the desired behavior.



**Figure(5.11):** Stateflow Block.

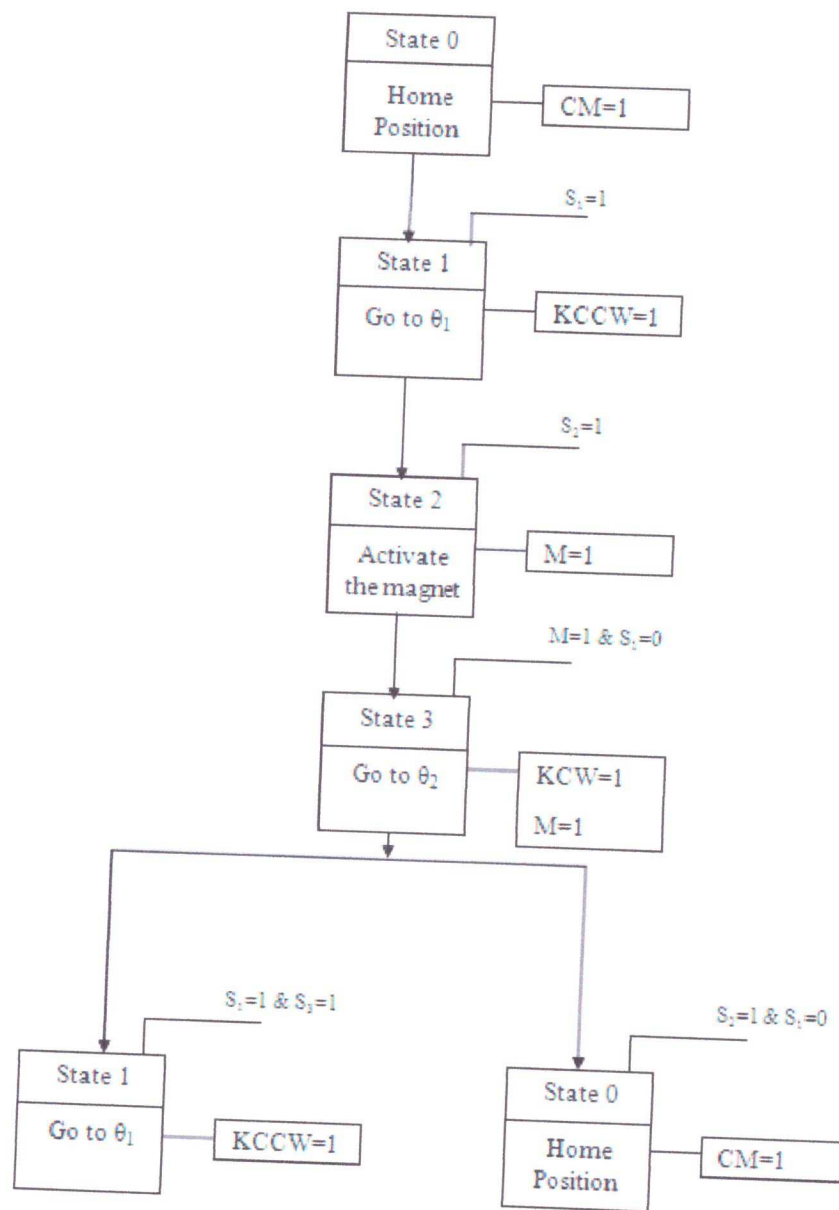
Every state is presented by a block; this block shows what is running at that state. On the other hand, the conditions needed are also shown (figure (5.9))

#### 5.4.2 Stateflow Diagram

In this section state flow diagram will be built as sequential blocks to determine synchronized control in each operation and then a brief description of the operations shown to explain what will happen in each state. To build the stateflow the inputs (conditions) and the outputs symbolized as shown in table(5.1).

**Table(5.1):** Symbolizing stateflow variables.

Conditions	Outputs
$S_1$ : proximity sensor. $S_1=1$ ; there is a part.	CM: conveyor motor CM=1; conveyor motor is activated
$S_2$ : potentiometer sensor. $S_2=1$ ; $\theta_1$ is reached. $\theta_1$ : position of crane over the part.	M: magnet. M=1; magnet is activated.
$S_3$ : potentiometer sensor. $S_3=1$ ; $\theta_2$ is reached. $\theta_2$ : position of crane to put the part.	KCCW: crane motor moves counter clock wise KCCW=1; crane moves CCW. KCW: crane motor moves clock wise. KCW=1; crane moves CW.



Figure(5.12): The Stateflow

Simulink program is shown in appendix B.

## **Chapter Six**

### **Results and Recommendation**

#### **6.1 Introduction**

This chapter contains the results that are obtained from the experiments which are done to verify the theoretical results reached in the previous chapters, where the mechanical, electrical, and control designs are to be applied in the practical side. The practical results and modifications that are done to the theoretical results are discussed.

A group of suggestions and recommendations are provided to enhance the performance of the system especially at the control field. Also the problems that faced the working team will be expressed.

## 6.2 Practical Results

### 6.2.1 Practical Mechanical results

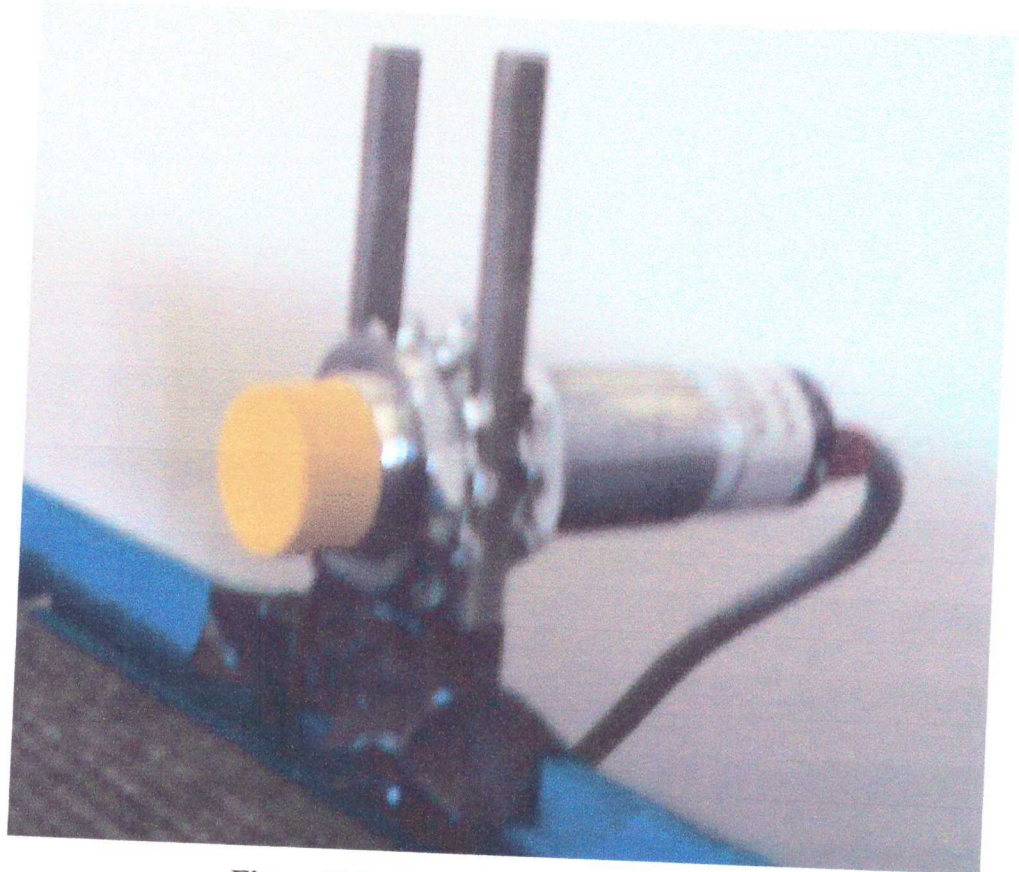
- 1) In this project, translational motion along the boom of the jib crane is neglected because it is very slow relatively; due to the screw mechanism (the pitch distance is very small) it must be another mechanism.
- 2) A magnet is hanged to the cable of the hoist so as to pull up the part from the conveyor is very strong, so when it pulls the part a undesired vibration occurs.



**Figure(6.1):** The magnet.



- 3) The proximity (inductive proximity sensor) sensor mounted on the conveyer to detect the coming parts, affected by the magnet to cancel this effect the magnet must be enough far from the sensor, so the correct reading from the sensor can be obtained.



**Figure(6.2):** Inductive proximity sensor.

- 4) The cable hoist has been fixed at a constant length which is above the conveyer with a suitable distance between the magnet and the part, also the cable length is governed by the mathematical model of the jib crane that consider the length cable is constant. The transportation of the part will be to a desired position that have the same height as the conveyer, in this way the automation time will be reduced and the system will be more efficient.

### 6.2.2 Practical Electrical results

The most important test in the electrical domain is the driving circuit that it was implemented in the university and especially in the Computer control system lab by the benefit of Eng.Khaled Tamizi.

This circuit amplifies the output current from the DAQ(Data Acquisition card), as it known that the DAQ current is relatively small so it can't drive a motor, so this circuit is responsible to give a current gain to drive the rotational motor of the jib crane.

### 6.2.3 Practical control results

- 1) Replacing an Ac motor with a Dc motor so the control operation will be more easier and to estimate a position control for the rotational motor of the jib crane.
- 2) Steady state error of the rotational angle is not zero in reality although using the PID controller because of the friction(non-linear term) and the elasticity of the chain that connect between the gear and the second gear that is mounted to the shaft of the rotational motor.
- 3) The Dc-motor that have been placed in the jib crane receives a voltage signal instead of torque signal unlike servo motors, therefore the states of the system could not be controlled to achieve the principles of the advanced control(Regulation, tracking input.....etc).

- 4) As it mentioned in chapter five, mechanical disturbance rejection is applied to the system by the mean of a worm gear, so any disturbance will be eliminated.

### 6.3 Recommendation

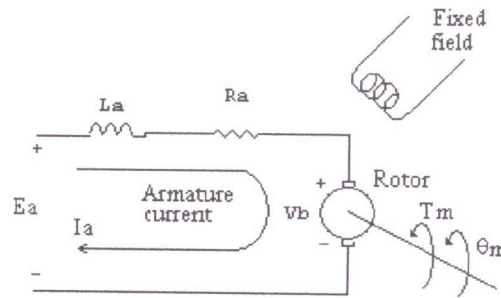
During the theoretical and practical working, a lot of problems faced the working team throughout all the project stages. The first problem is in the very small and the unsafe place that the university have chosen it for the working team to complete the practical work in it. As it known that this project need at least  $9m^2$  area and a good electricity network to be able to interface the two mechanical systems., so the team recommends to offer a suitable work station computer to perform such tasks.

At the practical side, most of the problems that faced the working team in eliminating the vibration of the cable of the hoist, the oscillation of the load is high relatively during the motion of the jib crane and during the lifting operation by the magnet, so the working team recommends to bring a servo motors to eliminate the vibration of the cable and to provide a control torque signal.

The working team recommends developing the system to be fully controlled for the three degree of freedom motions: rotation, translation, and hoisting, this is done by the existence of three servo motors that works simultaneously.

**Appendix A: Rotational-motion DC motor transfer function  
Identification**

The used motor for rotational motion is a permanent magnet DC motor. A motor is an electromechanical component that yields a displacement output for a voltage input that is a mechanical output generated by an electrical input. The motor schematic is shown in figure(A.1).



**Figure(A.1):** The motor schematic.

To derive the transfer function of this system, the relations between the electrical parameters and the mechanical parameters must be known. The voltage is proportional to the speed; Thus,

$$V_b = K_b \frac{d\theta_m(t)}{dt} \quad (\text{A.1})$$

Taking Laplace transform, we get

$$V_b = K_b s \theta_m(s) \quad (\text{A.2})$$

On the other hand, the torque developed by the motor is proportional to the armature current; thus,

$$T_m(s) = K_t I_a(s) \quad (\text{A.3})$$

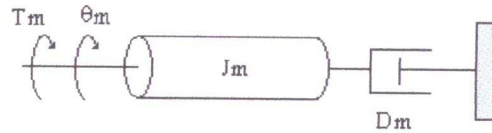
The loop equation around the armature circuit is

$$R_a I_a(s) + L_a s I_a(s) + V_b(s) = E_a(s) \quad (\text{A.4})$$

Substituting equations (A.2) and (A.3) into (A.4) yields

$$\frac{(R_a + L_a s)T_m(s)}{K_t} + K_b s \theta_m = E_a(s) \quad (\text{A.5})$$

Now the  $T_m(s)$  must be found in terms of  $\theta_m(s)$ , a typical equivalent mechanical load is shown in figure (A.2).



**Figure(A.2):** a typical equivalent mechanical load

From the figure(A.2)

$$T_m(s) = (J_m s^2 + D_m s) \theta_m(s) \quad (\text{A.6})$$

Substituting equation (A.6) into (A.5) and assuming that the armature inductance  $L_a$ , is smaller compared to the armature resistance  $R_a$ , yields

$$\left[ \frac{R_a}{K_t} (J_m s + D_m) + K_b \right] s \theta_m(s) = E_a(s) \quad (\text{A.7})$$

The desired transfer function  $\tilde{\theta}_m(s)/E_a(s)$ , is

$$\frac{\theta_m(s)}{T_m(s)} = \frac{K_t / R_a J_m}{s \left[ s + \frac{1}{J_m} \left( D_m + \frac{K_t K_b}{R_a} \right) \right]} \quad (\text{A.8})$$

The motor constants is given by

$$K_b = \frac{E_a}{\omega_{no-load}} \quad (\text{A.9})$$

$$K_t = \frac{T_{stall} R_a}{E_a} \quad (\text{A.10})$$

The motor constants can be found from torque-speed curve of the motor (figure (A.3)), the values of stall torque and no-load speed were found experimentally in the machines lab..

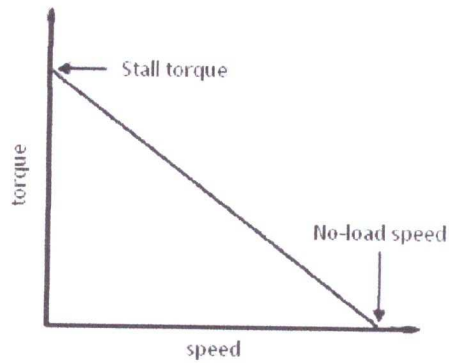


**Figure (A.3):** Torque-speed curve of a DC Motor.

**Table(A.1):** Experimental readings.

$\omega_m$ (rad/s)	38.7	33.5
$T_m$ (N.m)	0	0.1

The used DC motor was connected the break and control units in the lab., then two point in the torque-speed curve were taken(table(A.1)), the torque-speed relation is

$$\omega_m = 38.7 - 52.3T_m \quad (\text{A.9})$$

So the stall torque is 0.74 N.m and the no-load speed is 38.7 rad/s. the armature resistance was measured ( $R_a=18\Omega$ ), and the applied voltage,  $E_a$ , is 18V. So the motor constants are  $K_b=0.456$  V-s/rad and  $K_t=0.74$  N-m/A. The Load mass moment of inertia is known (section 3.2.2) and the damping is very small so it can be neglected, the transfer function is

$$G(s) = \frac{\theta_m(s)}{E_a(s)} = \frac{1}{s(s+0.5)} \quad (\text{A.10})$$

## **Appendix B: Control & Synchronization Simulink**



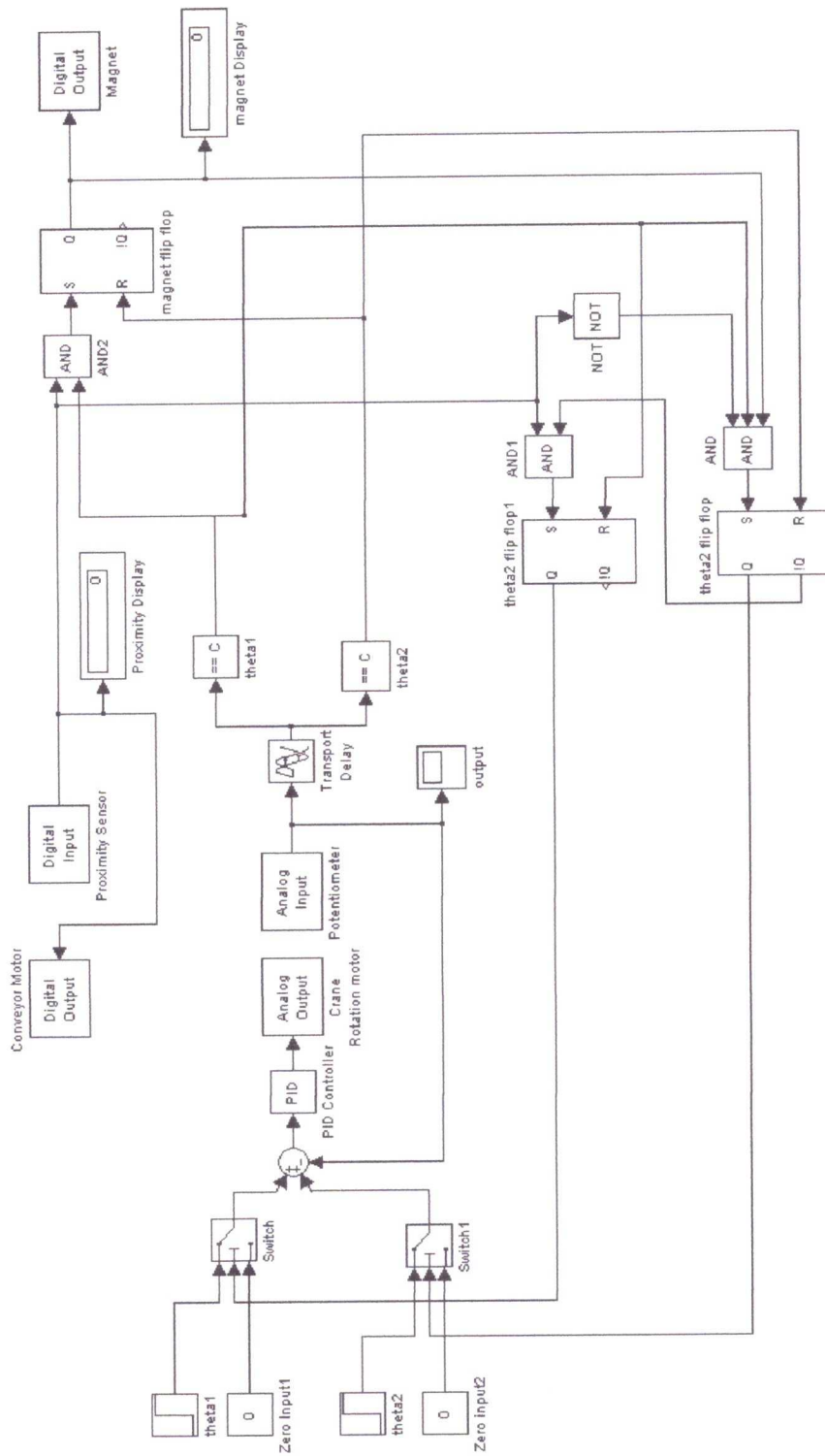


Figure (B.1): Simulink program.

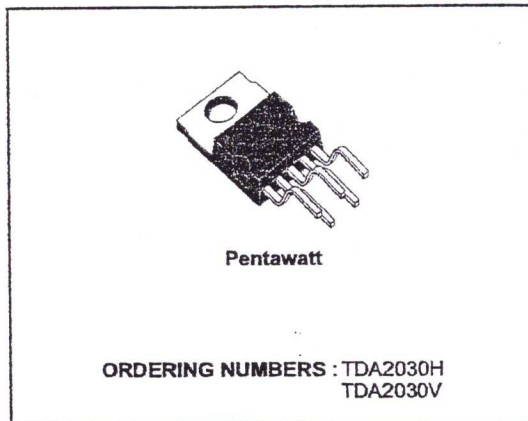
## **Appendix C: Datasheets for the used IC's**

## 14W Hi-Fi AUDIO AMPLIFIER

### DESCRIPTION

The TDA2030 is a monolithic integrated circuit in Pentawatt® package, intended for use as a low frequency class AB amplifier. Typically it provides 14W output power ( $d = 0.5\%$ ) at 14V/4Ω; at ±14V or 28V, the guaranteed output power is 12W on a 4Ω load and 8W on a 8Ω (DIN45500).

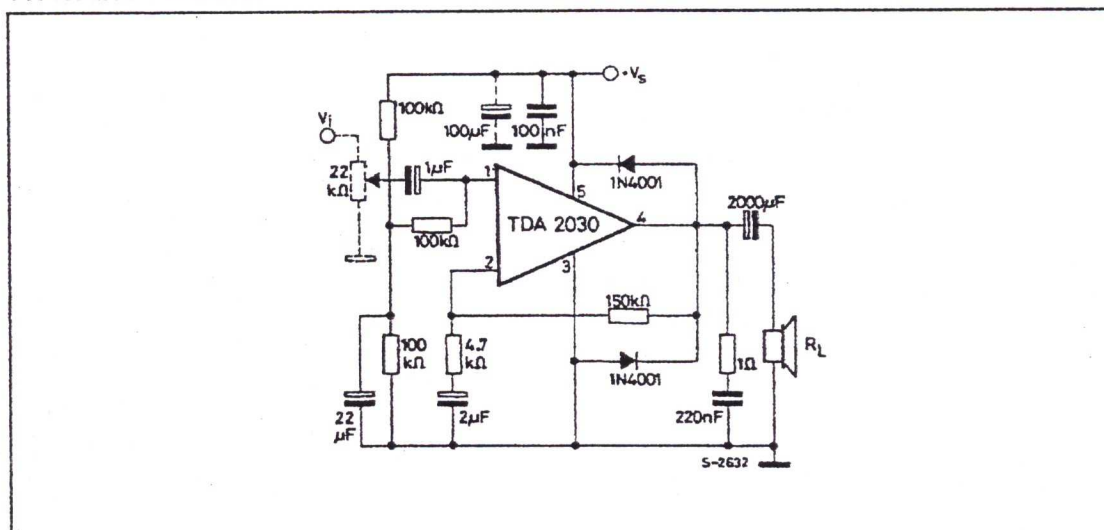
The TDA2030 provides high output current and has very low harmonic and cross-over distortion. Further the device incorporates an original (and patented) short circuit protection system comprising an arrangement for automatically limiting the dissipated power so as to keep the working point of the output transistors within their safe operating area. A conventional thermal shut-down system is also included.



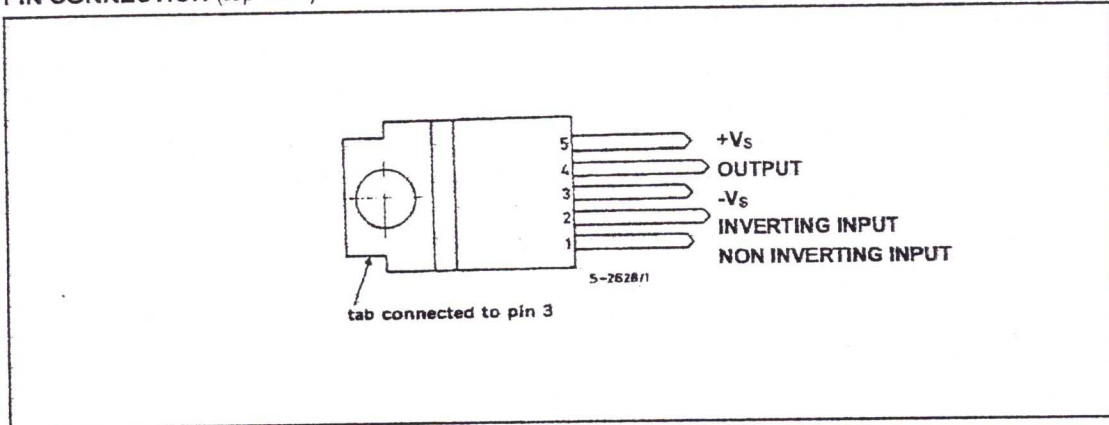
### ABSOLUTE MAXIMUM RATINGS

Symbol	Parameter	Value	Unit
$V_s$	Supply voltage	± 18 (36)	V
$V_i$	Input voltage	$V_s$	
$V_i$	Differential input voltage	± 15	V
$I_o$	Output peak current (internally limited)	3.5	A
$P_{tot}$	Power dissipation at $T_{case} = 90^\circ\text{C}$	20	W
$T_{slg}, T_j$	Storage and junction temperature	-40 to 150	$^\circ\text{C}$

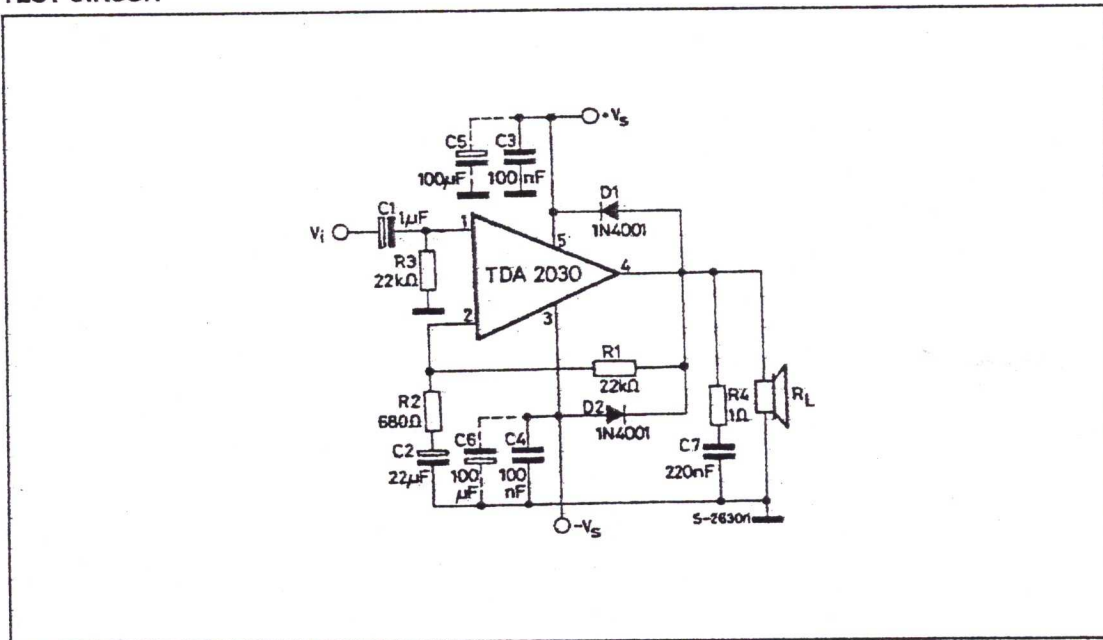
### TYPICAL APPLICATION



PIN CONNECTION (top view)



TEST CIRCUIT



## THERMAL DATA

Symbol	Parameter	Value	Unit
$R_{th\ j-case}$	Thermal resistance junction-case	max 3	$^{\circ}C/W$

**ELECTRICAL CHARACTERISTICS** (Refer to the test circuit,  $V_s = \pm 14V$ ,  $T_{amb} = 25^{\circ}C$  unless otherwise specified) for single Supply refer to fig. 15  $V_s = 28V$

Symbol	Parameter	Test conditions	Min.	Typ.	Max.	Unit
$V_s$	Supply voltage		$\pm 6$ 12		$\pm 18$ 36	V
$I_d$	Quiescent drain current	$V_s = \pm 18V$ ( $V_s = 36V$ )		40	60	mA
$I_b$	Input bias current			0.2	2	$\mu A$
$V_{os}$	Input offset voltage			$\pm 2$	$\pm 20$	mV
$I_{os}$	Input offset current			$\pm 20$	$\pm 200$	nA
$P_o$	Output power	$d = 0.5\%$ $G_v = 30\ dB$ $f = 40\ to\ 15,000\ Hz$ $R_L = 4\ \Omega$ $R_L = 8\ \Omega$	12 8	14 9		W W
		$d = 10\%$ $G_v = 30\ dB$ $f = 1\ KHz$ $R_L = 4\ \Omega$ $R_L = 8\ \Omega$		18 11		W W
d	Distortion	$P_o = 0.1\ to\ 12W$ $R_L = 4\ \Omega$ $G_v = 30\ dB$ $f = 40\ to\ 15,000\ Hz$		0.2	0.5	%
		$P_o = 0.1\ to\ 8W$ $R_L = 8\ \Omega$ $G_v = 30\ dB$ $f = 40\ to\ 15,000\ Hz$		0.1	0.5	%
B	Power Bandwidth (-3 dB)	$G_v = 30\ dB$ $P_o = 12W$ $R_L = 4\ \Omega$	10 to 140,000			Hz
$R_i$	Input resistance (pin 1)		0.5	5		$M\ \Omega$
$G_v$	Voltage gain (open loop)			90		dB
$G_v$	Voltage gain (closed loop)	$f = 1\ kHz$	29.5	30	30.5	dB
$e_N$	Input noise voltage	B = 22 Hz to 22 KHz		3	10	$\mu V$
$i_N$	Input noise current				80	200
SVR	Supply voltage rejection	$R_L = 4\ \Omega$ $G_v = 30\ dB$ $R_g = 22\ k\ \Omega$ $V_{ripple} = 0.5\ V_{eff}$ $f_{ripple} = 100\ Hz$	40	50		dB
$I_d$	Drain current	$P_o = 14W$ $R_L = 4\ \Omega$		900		mA
		$P_o = W$ $R_L = 8\ \Omega$		500		mA

Figure 1. Output power vs. supply voltage

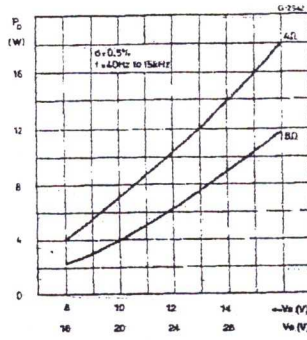


Figure 2. Output power vs. supply voltage

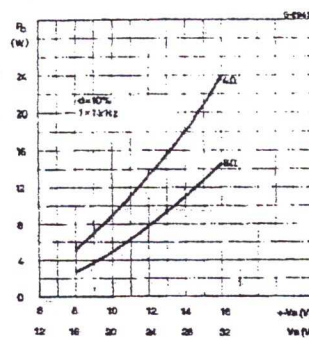


Figure 3. Distortion vs. output power

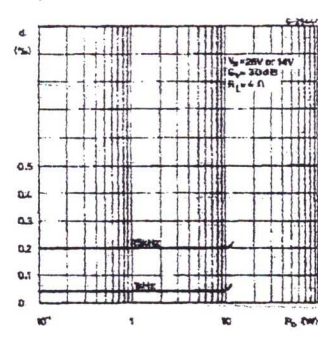


Figure 4. Distortion vs. output power

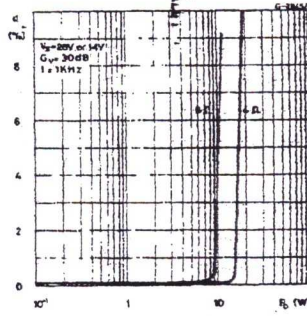


Figure 5. Distortion vs. output power

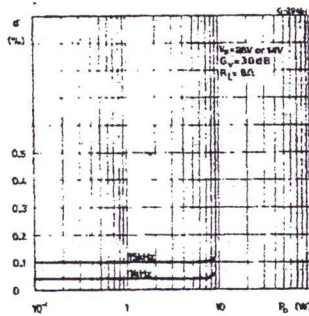


Figure 6. Distortion vs. frequency

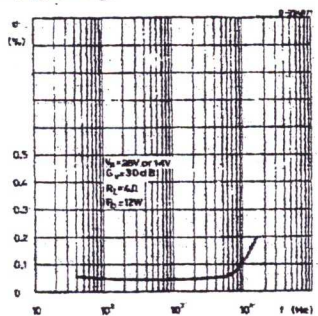


Figure 7. Distortion vs. frequency

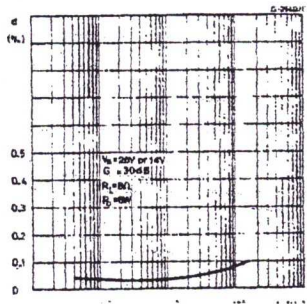


Figure 8. Frequency response with different values of the rolloff capacitor C8 (see fig. 13)

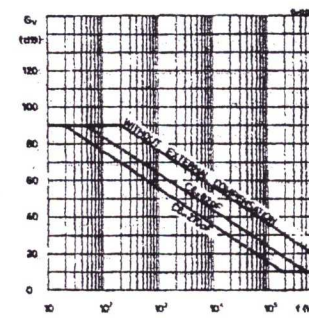
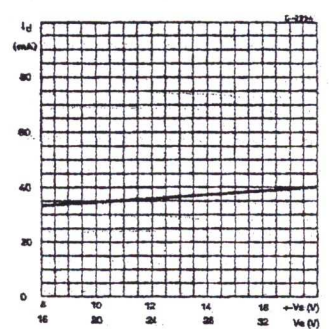


Figure 9. Quiescent current vs. supply voltage



APPLICATION INFORMATION (continued)

Figure 15. Typical amplifier with single power supply

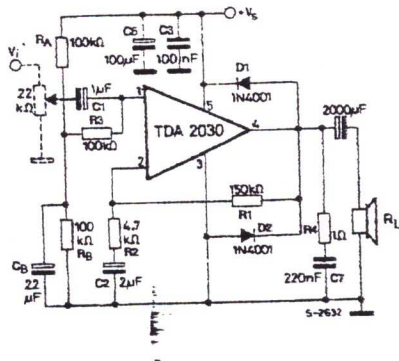


Figure 16. P.C. board and component layout for the circuit of fig. 15 (1 : 1 scale)

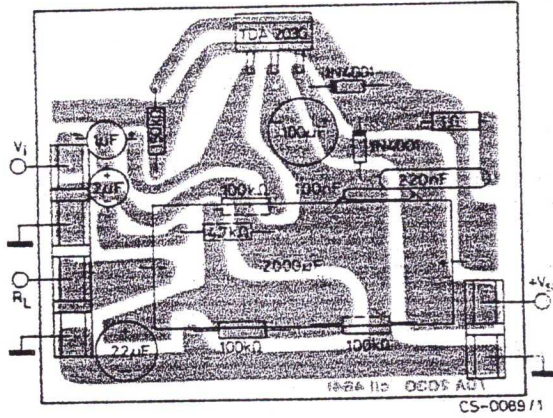
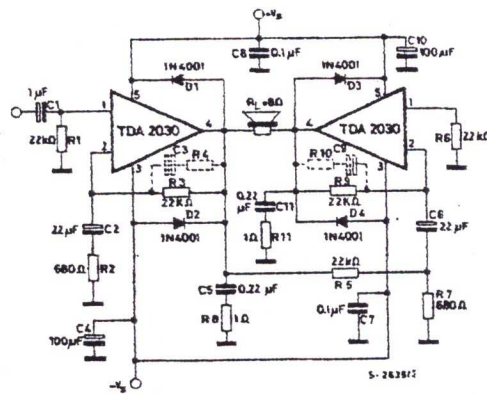


Figure 17. Bridge amplifier configuration with split power supply ( $P_o = 28W$ ,  $V_s = \pm 14V$ )



## PRACTICAL CONSIDERATIONS

**Printed circuit board**

The layout shown in Fig. 16 should be adopted by the designers. If different layouts are used, the ground points of input 1 and input 2 must be well decoupled from the ground return of the output in which a high current flows.

**Assembly suggestion**

No electrical isolation is needed between the

package and the heatsink with single supply voltage configuration.

**Application suggestions**

The recommended values of the components are those shown on application circuit of fig. 13. Different values can be used. The following table can help the designer.

Component	Recomm. value	Purpose	Larger than recommended value	Smaller than recommended value
R1	22 k $\Omega$	Closed loop gain setting	Increase of gain	Decrease of gain (*)
R2	680 $\Omega$	Closed loop gain setting	Decrease of gain (*)	Increase of gain
R3	22 k $\Omega$	Non inverting input biasing	Increase of input impedance	Decrease of input impedance
R4	1 $\Omega$	Frequency stability	Danger of oscillat. at high frequencies with induct. loads	
R5	$\cong 3 R2$	Upper frequency cutoff	Poor high frequencies attenuation	Danger of oscillation
C1	1 $\mu\text{F}$	Input DC decoupling		Increase of low frequencies cutoff
C2	22 $\mu\text{F}$	Inverting DC decoupling		Increase of low frequencies cutoff
C3, C4	0.1 $\mu\text{F}$	Supply voltage bypass		Danger of oscillation
C5, C6	100 $\mu\text{F}$	Supply voltage bypass		Danger of oscillation
C7	0.22 $\mu\text{F}$	Frequency stability		Danger of oscillation
C8	$\cong \frac{1}{2\pi B R1}$	Upper frequency cutoff	Smaller bandwidth	Larger bandwidth
D1, D2	1N4001	To protect the device against output voltage spikes		

(\*) Closed loop gain must be higher than 24dB



## SINGLE SUPPLY APPLICATION

Component	Recomm. value	Purpose	Larger than recommended value	Smaller than recommended value
R1	150 k $\Omega$	Closed loop gain setting	Increase of gain	Decrease of gain (*)
R2	4.7 k $\Omega$	Closed loop gain setting	Decrease of gain (*)	Increase of gain
R3	100 k $\Omega$	Non inverting input biasing	Increase of input impedance	Decrease of input impedance
R4	1 $\Omega$	Frequency stability	Danger of oscillat. at high frequencies with induct. loads	
R <sub>A</sub> /R <sub>B</sub>	100 k $\Omega$	Non inverting input Biasing		Power Consumption
C1	1 $\mu$ F	Input DC decoupling		Increase of low frequencies cutoff
C2	22 $\mu$ F	Inverting DC decoupling		Increase of low frequencies cutoff
C3	0.1 $\mu$ F	Supply voltage bypass		Danger of oscillation
C5	100 $\mu$ F	Supply voltage bypass		Danger of oscillation
C7	0.22 $\mu$ F	Frequency stability		Danger of oscillation
C8	$\cong \frac{1}{2\pi B R1}$	Upper frequency cutoff	Smaller bandwidth	Larger bandwidth
D1, D2	1N4001	To protect the device against output voltage spikes		

(\*) Closed loop gain must be higher than 24dB

## SINGLE SUPPLY APPLICATION

Component	Recomm. value	Purpose	Larger than recommended value	Smaller than recommended value
R1	150 k $\Omega$	Closed loop gain setting	Increase of gain	Decrease of gain (*)
R2	4.7 k $\Omega$	Closed loop gain setting	Decrease of gain (*)	Increase of gain
R3	100 k $\Omega$	Non inverting input biasing	Increase of input impedance	Decrease of input impedance
R4	1 $\Omega$	Frequency stability	Danger of oscillat. at high frequencies with induct. loads	
R <sub>A</sub> /R <sub>B</sub>	100 k $\Omega$	Non inverting input Biasing		Power Consumption
C1	1 $\mu$ F	Input DC decoupling		Increase of low frequencies cutoff
C2	22 $\mu$ F	Inverting DC decoupling		Increase of low frequencies cutoff
C3	0.1 $\mu$ F	Supply voltage bypass		Danger of oscillation
C5	100 $\mu$ F	Supply voltage bypass		Danger of oscillation
C7	0.22 $\mu$ F	Frequency stability		Danger of oscillation
C8	$\approx \frac{1}{2\pi B R1}$	Upper frequency cutoff	Smaller bandwidth	Larger bandwidth
D1, D2	1N4001	To protect the device against output voltage spikes		

(\*) Closed loop gain must be higher than 24dB

## SINGLE SUPPLY APPLICATION

Component	Recomm. value	Purpose	Larger than recommended value	Smaller than recommended value
R1	150 k $\Omega$	Closed loop gain setting	Increase of gain	Decrease of gain (*)
R2	4.7 k $\Omega$	Closed loop gain setting	Decrease of gain (*)	Increase of gain
R3	100 k $\Omega$	Non inverting input biasing	Increase of input impedance	Decrease of input impedance
R4	1 $\Omega$	Frequency stability	Danger of oscillat. at high frequencies with induct. loads	
R <sub>A</sub> /R <sub>B</sub>	100 k $\Omega$	Non inverting input Biasing		Power Consumption
C1	1 $\mu$ F	Input DC decoupling		Increase of low frequencies cutoff
C2	22 $\mu$ F	Inverting DC decoupling		Increase of low frequencies cutoff
C3	0.1 $\mu$ F	Supply voltage bypass		Danger of oscillation
C5	100 $\mu$ F	Supply voltage bypass		Danger of oscillation
C7	0.22 $\mu$ F	Frequency stability		Danger of oscillation
C8	$\cong \frac{1}{2\pi B R1}$	Upper frequency cutoff	Smaller bandwidth	Larger bandwidth
D1, D2	1N4001	To protect the device against output voltage spikes		

(\*) Closed loop gain must be higher than 24dB

## SHORT CIRCUIT PROTECTION

The TDA2030 has an original circuit which limits the current of the output transistors. Fig. 18 shows that the maximum output current is a function of the collector emitter voltage; hence the output transistors work within their safe operating area (Fig. 2). This function can therefore be considered as being

peak power limiting rather than simple current limiting. It reduces the possibility that the device gets damaged during an accidental short circuit from AC output to ground.

Figure 18. Maximum output current vs. voltage [ $V_{CEsat}$ ] across each output transistor

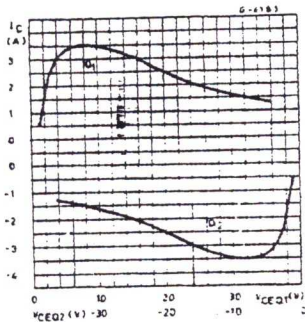
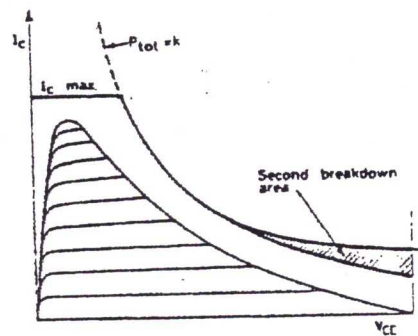


Figure 19. Safe operating area and collector characteristics of the protected power transistor



## THERMAL SHUT-DOWN

The presence of a thermal limiting circuit offers the following advantages:

1. An overload on the output (even if it is permanent), or an above limit ambient temperature can be easily supported since the  $T_j$  cannot be higher than  $150^\circ\text{C}$ .
2. The heatsink can have a smaller factor of safety compared with that of a conventional circuit. There is no possibility of device damage due to high junction temperature. If for any reason, the

junction temperature increases up to  $150^\circ\text{C}$ , the thermal shut-down simply reduces the power dissipation at the current consumption.

The maximum allowable power dissipation depends upon the size of the external heatsink (i.e. its thermal resistance); fig. 22 shows this dissippable power as a function of ambient temperature for different thermal resistance.

Figure 20. Output power and drain current vs. case temperature ( $R_L = 4\Omega$ )

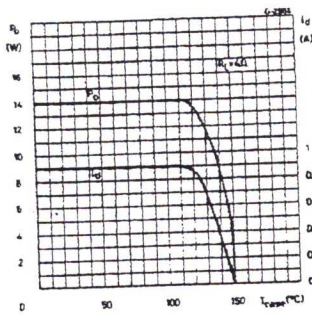


Figure 21. Output power and drain current vs. case temperature ( $R_L = 8\Omega$ )

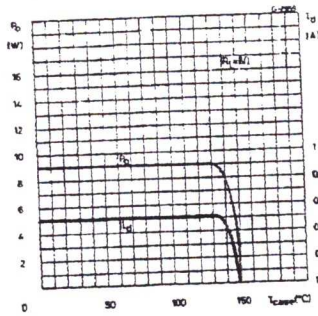


Figure 22. Maximum allowable power dissipation vs. ambient temperature

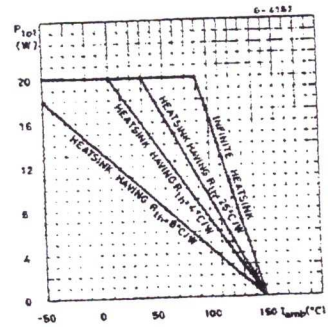
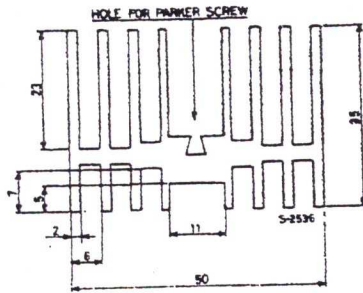


Figure 23. Example of heat-sink



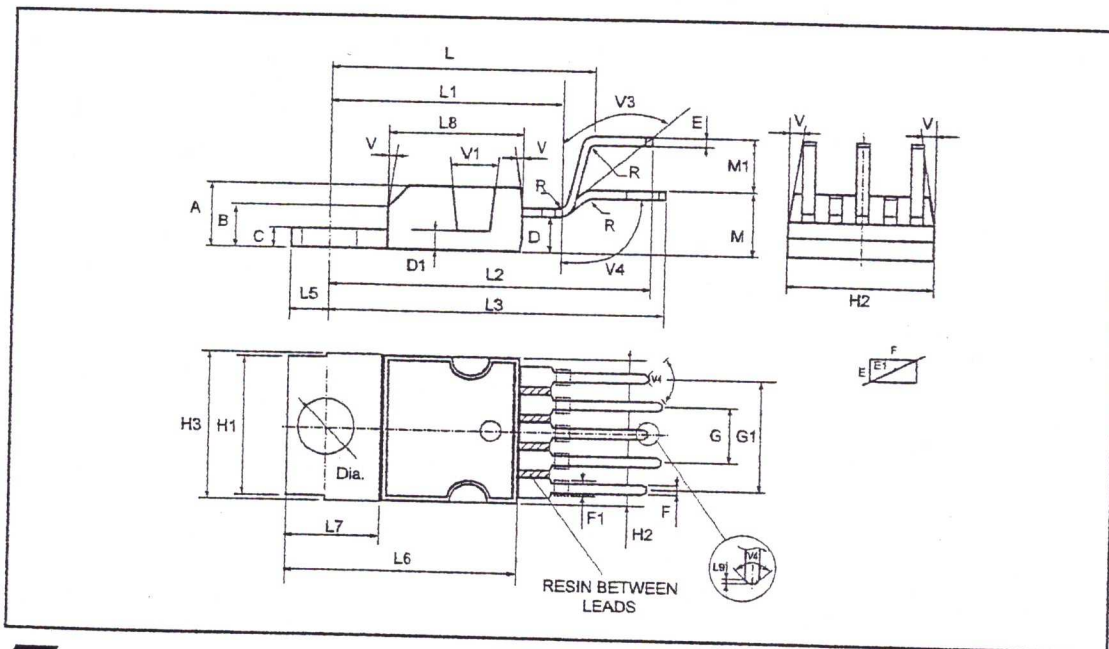
Dimension : suggestion.

The following table shows the length that the heatsink in fig. 23 must have for several values of  $P_{tot}$  and  $R_{th}$ .

$P_{tot}$ (W)	12	8	6
Length of heatsink (mm)	60	40	30
$R_{th}$ of heatsink ( $^{\circ}C/W$ )	4.2	6.2	8.3

PENTAWATT PACKAGE MECHANICAL DATA

DIM.	mm			inch		
	MIN.	TYP.	MAX.	MIN.	TYP.	MAX.
A			4.8			0.189
C			1.37			0.054
D	2.4		2.8	0.094		0.110
D1	1.2		1.35	0.047		0.053
E	0.35		0.55	0.014		0.022
E1	0.76		1.19	0.030		0.047
F	0.8		1.05	0.031		0.041
F1	1		1.4	0.039		0.055
G	3.2	3.4	3.6	0.126	0.134	0.142
G1	6.6	6.8	7	0.260	0.268	0.276
H2			10.4			0.409
H3	10.05		10.4	0.396		0.409
L	17.55	17.85	18.15	0.691	0.703	0.715
L1	15.55	15.75	15.95	0.612	0.620	0.628
L2	21.2	21.4	21.6	0.831	0.843	0.850
L3	22.3	22.5	22.7	0.878	0.886	0.894
L4			1.29			0.051
L5	2.6		3	0.102		0.118
L6	15.1		15.8	0.594		0.622
L7	6		6.6	0.236		0.260
L9		0.2			0.008	
M	4.23	4.5	4.75	0.167	0.177	0.187
M1	3.75	4	4.25	0.148	0.157	0.167
V4	40° (typ.)					
Dia	3.65		3.85	0.144		0.152



Information furnished is believed to be accurate and reliable. However, STMicroelectronics assumes no responsibility for the consequences of use of such information nor for any infringement of patents or other rights of third parties which may result from its use. No license is granted by implication or otherwise under any patent or patent rights of STMicroelectronics. Specification mentioned in this publication are subject to change without notice. This publication supersedes and replaces all information previously supplied. STMicroelectronics products are not authorized for use as critical components in life support devices or systems without express written approval of STMicroelectronics.

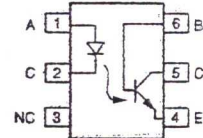
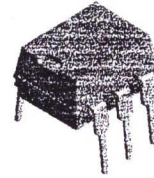
The ST logo is a registered trademark of STMicroelectronics  
© 1998 STMicroelectronics - Printed in Italy - All Rights Reserved  
STMicroelectronics GROUP OF COMPANIES

Australia - Brazil - Canada - China - France - Germany - Italy - Japan - Korea - Malaysia - Malta - Mexico - Morocco - The Netherlands - Singapore - Spain - Sweden - Switzerland - Taiwan - Thailand - United Kingdom - U.S.A.

## Optocoupler, Phototransistor Output, With Base Connection

### Features

- Isolation Test Voltage 5300 V<sub>RMS</sub>
- Interfaces with Common Logic Families
- Input-output Coupling Capacitance < 0.5 pF
- Industry Standard Dual-in-line 6-pin Package
- Lead-free component
- Component in accordance to RoHS 2002/95/EC and WEEE 2002/96/EC



### Agency Approvals

- UL1577, File No. E52744 System Code H or J, Double Protection
- DIN EN 60747-5-2 (VDE0884)  
DIN EN 60747-5-5 pending  
Available with Option 1

### Applications

AC Mains Detection  
 Reed relay driving  
 Switch Mode Power Supply Feedback  
 Telephone Ring Detection  
 Logic Ground Isolation  
 Logic Coupling with High Frequency Noise Rejection

### Description

The 4N25 family is an Industry Standard Single Channel Phototransistor Coupler. This family includes the 4N25/ 4N26/ 4N27/ 4N28. Each optocoupler consists of gallium arsenide infrared LED and a silicon NPN phototransistor.

These couplers are Underwriters Laboratories (UL) listed to comply with a 5300 V<sub>RMS</sub> isolation test voltage. This isolation performance is accomplished through special Vishay manufacturing process.

Compliance to DIN EN 60747-5-2(VDE0884)/ DIN EN 60747-5-5 pending partial discharge isolation specification is available by ordering option 1.

These isolation processes and the Vishay ISO9001 quality program results in the highest isolation performance available for a commercial plastic phototransistor optocoupler.

The devices are also available in lead formed configuration suitable for surface mounting and are available either on tape and reel, or in standard tube shipping containers.

#### Note:

For additional design information see Application Note 45 Normalized Curves

### Order Information

Part	Remarks
4N25	CTR > 20 %, DIP-6
4N26	CTR > 20 %, DIP-6
4N27	CTR > 10 %, DIP-6
4N28	CTR > 10 %, DIP-6
4N25-X006	CTR > 20 %, DIP-6 400 mil (option 6)
4N25-X007	CTR > 20 %, SMD-6 (option 7)
4N25-X009	CTR > 20 %, SMD-6 (option 9)
4N26-X006	CTR > 20 %, DIP-6 400 mil (option 6)
4N26-X007	CTR > 20 %, SMD-6 (option 7)
4N26-X009	CTR > 20 %, SMD-6 (option 9)
4N27-X007	CTR > 10 %, SMD-6 (option 7)
4N27-X009	CTR > 10 %, SMD-6 (option 9)
4N28-X009	CTR > 10 %, SMD-6 (option 9)

For additional information on the available options refer to Option Information.



### Absolute Maximum Ratings

$T_{amb} = 25\text{ }^{\circ}\text{C}$ , unless otherwise specified

Stresses in excess of the absolute Maximum Ratings can cause permanent damage to the device. Functional operation of the device is not implied at these or any other conditions in excess of those given in the operational sections of this document. Exposure to absolute Maximum Rating for extended periods of the time can adversely affect reliability.

### Input

Parameter	Test condition	Symbol	Value	Unit
Reverse voltage		$V_R$	6.0	V
Forward current		$I_F$	60	mA
Surge current	$t < 10\text{ }\mu\text{s}$	$I_{FSM}$	2.5	A
Power dissipation		$P_{diss}$	100	mW

### Output

Parameter	Test condition	Symbol	Value	Unit
Collector-emitter breakdown voltage		$V_{CEO}$	70	V
Emitter-base breakdown voltage		$V_{EBO}$	7.0	V
Collector current		$I_C$	50	mA
Collector current	$t < 1.0\text{ ms}$	$I_C$	100	mA
Power dissipation		$P_{diss}$	150	mW

### Coupler

Parameter	Test condition	Symbol	Value	Unit
Isolation test voltage		$V_{ISO}$	5300	$V_{RMS}$
Creepage			$\geq 7.0$	mm
Clearance			$\geq 7.0$	mm
Isolation thickness between emitter and detector			$\geq 0.4$	mm
Comparative tracking index	DIN IEC 112/VDE0303, part 1		175	
Isolation resistance	$V_{IO} = 500\text{ V}$ , $T_{amb} = 25\text{ }^{\circ}\text{C}$	$R_{IO}$	$10^{12}$	$\Omega$
	$V_{IO} = 500\text{ V}$ , $T_{amb} = 100\text{ }^{\circ}\text{C}$	$R_{IO}$	$10^{11}$	$\Omega$
Storage temperature		$T_{stg}$	- 55 to + 150	$^{\circ}\text{C}$
Operating temperature		$T_{amb}$	- 55 to + 100	$^{\circ}\text{C}$
Junction temperature		$T_j$	100	$^{\circ}\text{C}$
Soldering temperature	max. 10 s, dip soldering: distance to seating plane $\geq 1.5\text{ mm}$	$T_{sld}$	260	$^{\circ}\text{C}$



**Electrical Characteristics**

T<sub>amb</sub> = 25 °C, unless otherwise specified

Minimum and maximum values are testing requirements. Typical values are characteristics of the device and are the result of engineering evaluation. Typical values are for information only and are not part of the testing requirements.

**Input**

Parameter	Test condition	Symbol	Min	Typ.	Max	Unit
Forward voltage <sup>1)</sup>	I <sub>F</sub> = 50 mA	V <sub>F</sub>		1.3	1.5	V
Reverse current <sup>1)</sup>	V <sub>R</sub> = 3.0 V	I <sub>R</sub>		0.1	100	μA
Capacitance	V <sub>R</sub> = 0 V	C <sub>O</sub>		25		pF

<sup>1)</sup> Indicates JEDEC registered values

**Output**

Parameter	Test condition	Part	Symbol	Min	Typ.	Max	Unit
Collector-base breakdown voltage <sup>1)</sup>	I <sub>C</sub> = 100 μA		BV <sub>CBO</sub>	70			V
Collector-emitter breakdown voltage <sup>1)</sup>	I <sub>C</sub> = 1.0 mA		BV <sub>CEO</sub>	30			V
Emitter-collector breakdown voltage <sup>1)</sup>	I <sub>E</sub> = 100 μA		BV <sub>ECO</sub>	7.0			V
I <sub>CEO</sub> (dark) <sup>1)</sup>	V <sub>CE</sub> = 10 V, (base open)	4N25			5.0	50	nA
		4N26			5.0	50	nA
		4N27			5.0	50	nA
		4N28			10	100	nA
I <sub>CBO</sub> (dark) <sup>1)</sup>	V <sub>CB</sub> = 10 V, (emitter open)				2.0	20	nA
Collector-emitter capacitance	V <sub>CE</sub> = 0		C <sub>CE</sub>		6.0		pF

<sup>1)</sup> Indicates JEDEC registered values

**Coupler**

Parameter	Test condition	Part	Symbol	Min	Typ.	Max	Unit
Isolation voltage <sup>1)</sup>	Peak, 60 Hz	4N25	V <sub>IO</sub>	2500			V
		4N26	V <sub>IO</sub>	1500			V
		4N27	V <sub>IO</sub>	1500			V
		4N28	V <sub>IO</sub>	500			V
Saturation voltage, collector-emitter	I <sub>CE</sub> = 2.0 mA, I <sub>F</sub> = 50 mA		V <sub>CE(sat)</sub>			0.5	V
Resistance, input output <sup>1)</sup>	V <sub>IO</sub> = 500 V		R <sub>IO</sub>	100			GΩ
Capacitance (input-output)	f = 1.0 MHz		C <sub>IO</sub>		0.5		pF

<sup>1)</sup> Indicates JEDEC registered values

**Current Transfer Ratio**

Parameter	Test condition	Part	Symbol	Min	Typ.	Max	Unit
DC Current Transfer Ratio <sup>1)</sup>	V <sub>CE</sub> = 10 V, I <sub>F</sub> = 10 mA	4N25	CTR <sub>DC</sub>	20	50		%
		4N26	CTR <sub>DC</sub>	20	50		%
		4N27	CTR <sub>DC</sub>	10	30		%
		4N28	CTR <sub>DC</sub>	10	30		%

<sup>1)</sup> Indicates JEDEC registered value

Switching Characteristics

Parameter	Test condition	Symbol	Min	Typ.	Max	Unit
Rise and fall times	$V_{CE} = 10\text{ V}$ , $I_F = 10\text{ mA}$ , $R_L = 100\ \Omega$	$t_r$ , $t_f$		2.0		$\mu\text{s}$

Typical Characteristics ( $T_{amb} = 25\text{ }^\circ\text{C}$  unless otherwise specified)

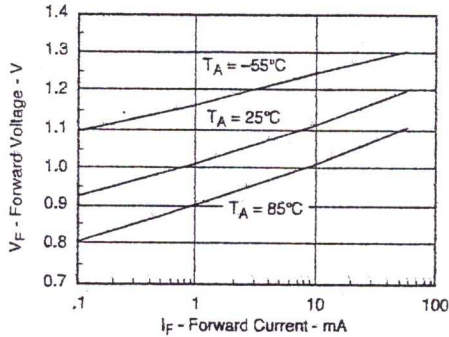


Figure 1. Forward Voltage vs. Forward Current

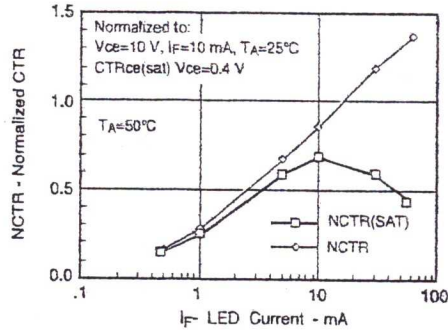


Figure 3. Normalized Non-saturated and Saturated CTR vs. LED Current

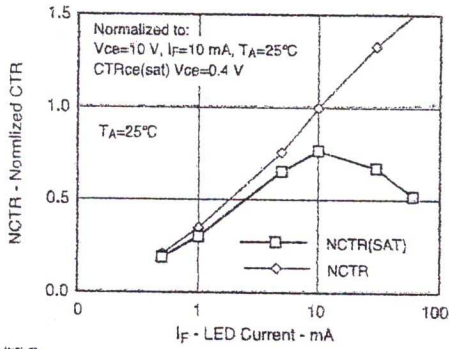


Figure 2. Normalized Non-Saturated and Saturated CTR vs. LED Current

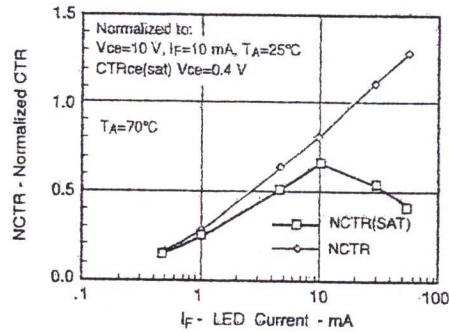


Figure 4. Normalized Non-saturated and saturated CTR vs. LED Current

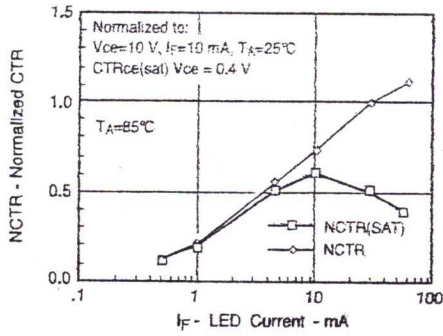


Figure 5. Normalized Non-saturated and saturated CTR vs. LED Current

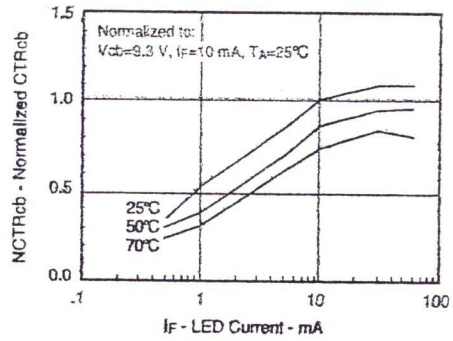


Figure 8. Normalized CTRcb vs. LED Current and Temp.

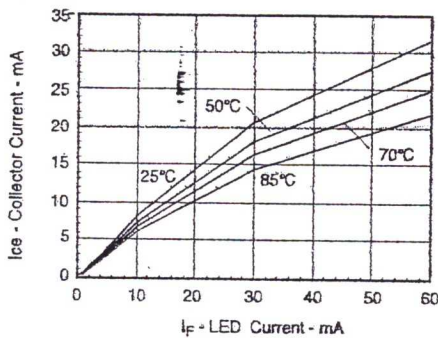


Figure 6. Collector-Emitter Current vs. Temperature and LED Current

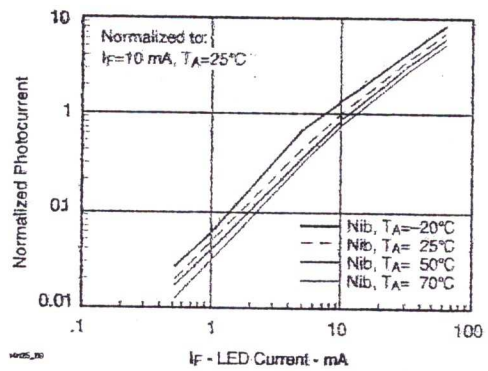


Figure 9. Normalized Photocurrent vs.  $I_F$  and Temp.

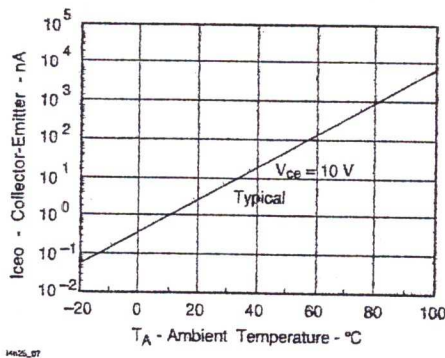


Figure 7. Collector-Emitter Leakage Current vs. Temp.

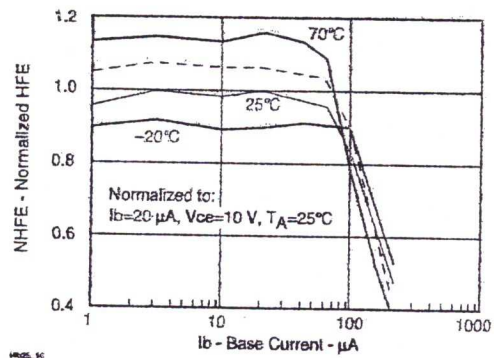


Figure 10. Normalized Non-saturated HFE vs. Base Current and Temperature

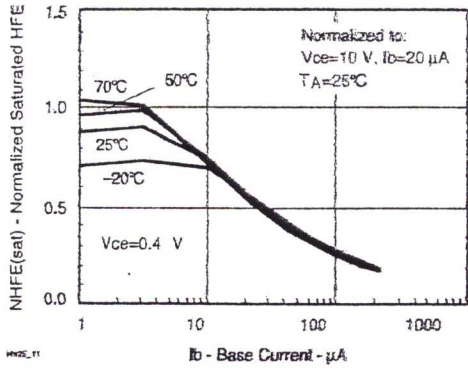


Figure 11. Normalized HFE vs. Base Current and Temp.

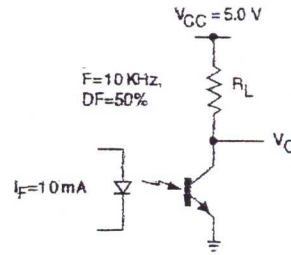


Figure 14. Switching Schematic

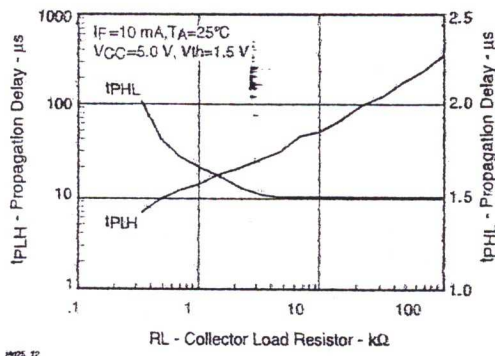


Figure 12. Propagation Delay vs. Collector Load Resistor

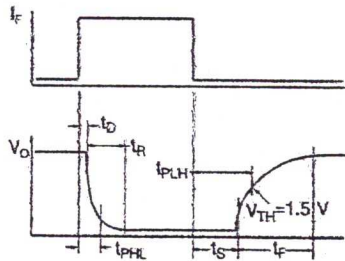


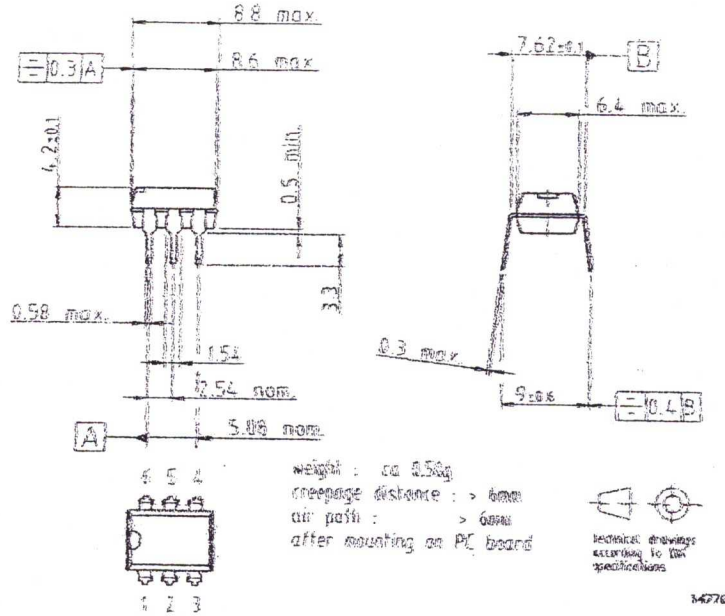
Figure 13. Switching Timing

## Package Dimensions in Inches (mm)

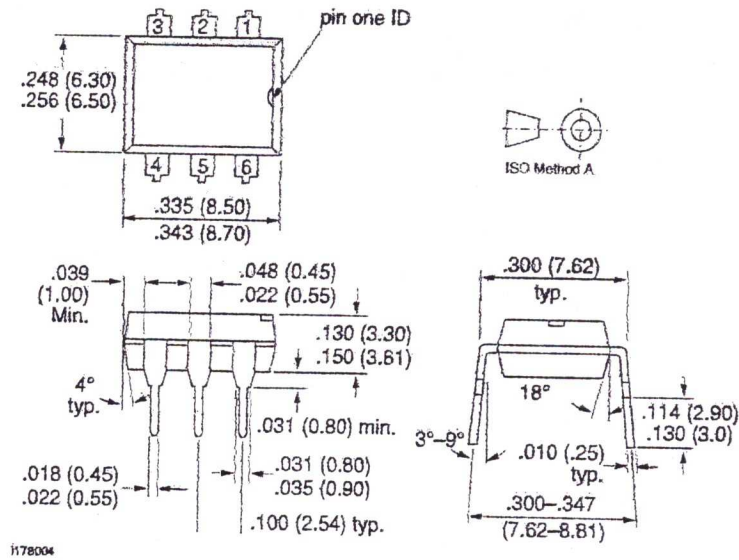
For 4N25/26/27..... see DIL300-6 Package dimension in the Package Section.

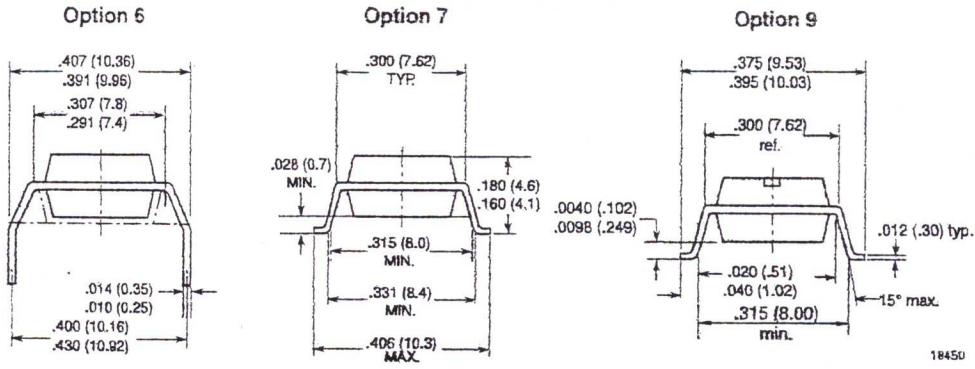
For 4N28 and for products with an option designator (e.g. 4N25-X001 or 4N26-X007)..... see DIP-6 Package dimensions in the Package Section.

### DIL300-6 Package Dimensions



### DIP-6 Package Dimensions







### Ozone Depleting Substances Policy Statement

It is the policy of Vishay Semiconductor GmbH to

1. Meet all present and future national and international statutory requirements.
2. Regularly and continuously improve the performance of our products, processes, distribution and operating systems with respect to their impact on the health and safety of our employees and the public, as well as their impact on the environment.

It is particular concern to control or eliminate releases of those substances into the atmosphere which are known as ozone depleting substances (ODSs).

The Montreal Protocol (1987) and its London Amendments (1990) intend to severely restrict the use of ODSs and forbid their use within the next ten years. Various national and international initiatives are pressing for an earlier ban on these substances.

Vishay Semiconductor GmbH has been able to use its policy of continuous improvements to eliminate the use of ODSs listed in the following documents.

1. Annex A, B and list of transitional substances of the Montreal Protocol and the London Amendments respectively
2. Class I and II ozone depleting substances in the Clean Air Act Amendments of 1990 by the Environmental Protection Agency (EPA) in the USA
3. Council Decision 88/540/EEC and 91/690/EEC Annex A, B and C (transitional substances) respectively.

Vishay Semiconductor GmbH can certify that our semiconductors are not manufactured with ozone depleting substances and do not contain such substances.

We reserve the right to make changes to improve technical design and may do so without further notice.

Parameters can vary in different applications. All operating parameters must be validated for each customer application by the customer. Should the buyer use Vishay Semiconductors products for any unintended or unauthorized application, the buyer shall indemnify Vishay Semiconductors against all claims, costs, damages, and expenses, arising out of, directly or indirectly, any claim of personal damage, injury or death associated with such unintended or unauthorized use.

Vishay Semiconductor GmbH, P.O.B. 3535, D-74025 Heilbronn, Germany  
Telephone: 49 (0)7131 67 2831, Fax number: 49 (0)7131 67 2423



## References

- [1] Ahmad Wajih Tahboub, Issa Abu Samra and Mohamad Tomizi, "Smart Conveyor", Palestine Polytechnic University, Palestine, 2006.
- [2] Ameen Al Jubah and Shareef Al Jubah, "Power Assisted Jib Crane", Palestine Polytechnic University, 2007.
- [3] Mikell P. Groover, Automation, production systems, and computer-integrated manufacturing, Prentice hall international, Inc, Lehigh university.
- [4] [www.wikipedia.com](http://www.wikipedia.com).
- [5] [www.everything2.com](http://www.everything2.com).
- [6] Harry M. Pearce, " The Design and Construction of an Intelligent Power Assist Jib Crane", Northwestern University, USA, 1999.
- [7] Norman S.Nise, Control Systems Engineering, fourth edition, California State Polytechnic Universty.